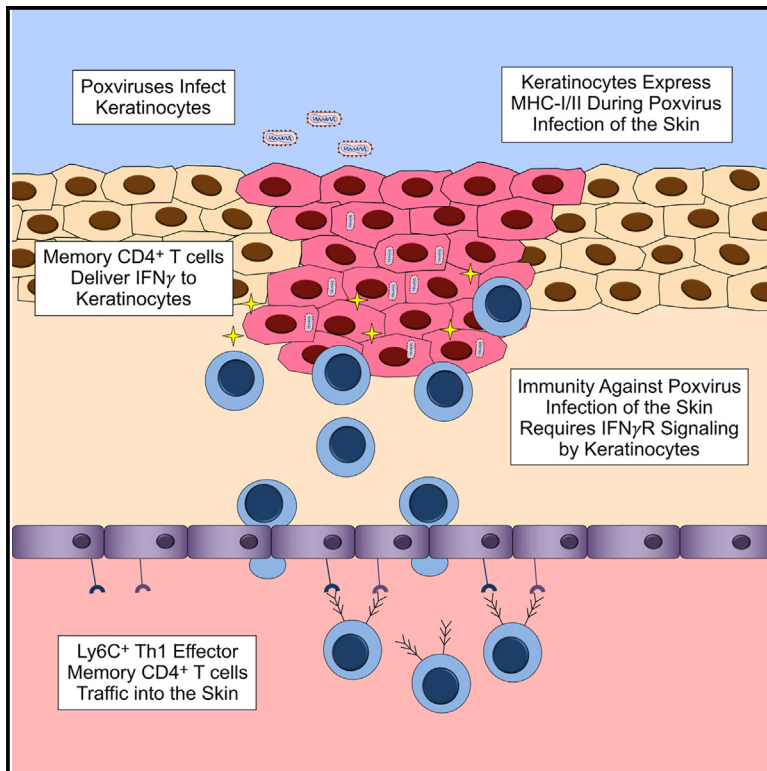# T helper 1 effector memory CD4+ T cells protect the skin from poxvirus infection

Graphical abstract

Authors

Jake C. Harbour, Mahmoud Abdelbary, John B. Schell, ..., Zheng Xia, Klaus Früh, Jeffrey C. Nolz

Correspondence

nolz@ohsu.edu

In brief

Poxvirus infections of the skin are an emerging public health concern, yet the mechanisms that are necessary to prevent these viral infections remain largely unknown. Here, Harbour et al. show that Th1 effector memory CD4+ T cells protect the skin from poxvirus infection by delivering IFNγ to keratinocytes.

Highlights

- Memory CD4+ T cells are sufficient to protect the skin from poxvirus infections

- Ly6C+ Th1 effector memory CD4+ T cells traffic into poxvirus-infected skin

- IFNγ causes keratinocytes to increase MHC class I/II expression during poxvirus infection

- Immunity against poxvirus skin infection requires IFNγR signaling by keratinocytes

Article

T helper 1 effector memory CD4⁺ T cells protect the skin from poxvirus infection

Jake C. Harbour,[1] Mahmoud Abdelbary,[1] John B. Schell,[2] Samantha P. Fancher,[1] Jack J. McLean,[1] Taylen J. Nappi,[1] Susan Liu,[3] Timothy J. Nice,[1] Zheng Xia,[3] Klaus Früh,[2] and Jeffrey C. Nolz[1,4,5,6,*]
[1]Department of Molecular Microbiology and Immunology, Oregon Health & Science University, Portland, OR, USA
[2]Vaccine and Gene Therapy Institute, Oregon Health & Science University, Beaverton, OR, USA
[3]Department of Biomedical Engineering, Oregon Health & Science University, Portland, OR, USA
[4]Department of Cell, Developmental and Cancer Biology, Oregon Health & Science University, Portland, OR, USA
[5]Department of Dermatology, Oregon Health & Science University, Portland, OR, USA
[6]Lead contact
*Correspondence: nolz@ohsu.edu
https://doi.org/10.1016/j.celrep.2023.112407

SUMMARY

Poxvirus infections of the skin are a recent emerging public health concern, yet the mechanisms that mediate protective immunity against these viral infections remain largely unknown. Here, we show that T helper 1 (Th1) memory CD4⁺ T cells are necessary and sufficient to provide complete and broad protection against poxvirus skin infections, whereas memory CD8⁺ T cells are dispensable. Core 2 O-glycan-synthesizing Th1 effector memory CD4⁺ T cells rapidly infiltrate the poxvirus-infected skin microenvironment and produce interferon γ (IFNγ) in an antigen-dependent manner, causing global changes in gene expression to promote anti-viral immunity. Keratinocytes express IFN-stimulated genes, upregulate both major histocompatibility complex (MHC) class I and MHC class II antigen presentation in an IFNγ-dependent manner, and require IFNγ receptor (IFNγR) signaling and MHC class II expression for memory CD4⁺ T cells to protect the skin from poxvirus infection. Thus, Th1 effector memory CD4⁺ T cells exhibit potent anti-viral activity within the skin, and keratinocytes are the key targets of IFNγ necessary for preventing poxvirus infection of the epidermis.

INTRODUCTION

Several viruses of the genus *Orthopoxvirus*, including vaccinia virus (VacV), cowpox virus (CPXV), and mpox, infect humans and are spread primarily through direct person-to-person or person-to-animal contact with infected skin lesions.[1,2] Variola virus, the causative agent of smallpox and also of the genus *Orthopoxvirus*, was eradicated from the planet through successful, wide-spread immunization with VacV, which generated poxvirus-specific neutralizing antibodies and memory T cells that persist in individuals even decades after receiving the vaccination.[3,4] Immunizations with VacV to protect against smallpox, in general, ended worldwide by 1980,[5,6] thus a large percentage of the world population no longer possesses pre-existing immunity against poxviruses, thereby rendering communities highly susceptible to widespread zoonotic poxvirus transmission.[7] In fact, between May and December 2022, there were >80,000 reported cases of mpox that spread to over 100 countries,[8,9] prompting the World Health Organization to declare the outbreak a public health emergency of international concern. Although vaccination campaigns have commenced using primarily the highly attenuated modified VacV Ankara (MVA) to combat mpox infection,[10,11] the mechanisms used by the adaptive immune system to protect against poxvirus infections of the skin and whether MVA vaccination will elicit the level and type of

immunological memory necessary to prevent the spread of zoonotic poxviruses remain largely unknown.

During their antigen-driven activation and clonal expansion, CD4⁺ T cells will differentiate into diverse lineages dependent on the activity of a number of cytokines that result in the expression of fate-defining transcription factors such as T-bet, GATA-3, and RORγt.[12] Following the resolution of viral infections, T-bet expressing, interferon γ (IFNγ)-producing T helper 1 (Th1) CD4⁺ T cells that survive contraction subsequently differentiate into memory cells that consist of Ly6C⁺/CCR7⁻ effector memory (T_EM), Ly6C⁻/CCR7⁺ central memory (T_CM), and PD-1⁺/CXCR5⁺ follicular helper (T_FH) memory,[13–15] but the mechanism(s) used by these diverse subsets to provide protection against virus re-infection remain ill defined. Prior studies using models of T cell transfer or depletion have provided evidence that CD4⁺ T cells can exhibit some level of anti-viral activity, both dependent and independent of their "helper" functions.[16] In fact, in-vitro-polarized, antigen-specific effector Th1 CD4⁺ T cells (but not Th2) migrate into inflammatory sites and provide protection against systemic VacV infection.[17] Zoonotic poxviruses such as CPXV and mpox express immune evasion genes that can inhibit major histocompatibility complex (MHC) class I antigen presentation,[18–20] thereby allowing these viruses to largely evade the direct anti-viral activity of cytotoxic CD8⁺ T cells.[21,22] Collectively, these findings raise the possibility that

Th1 CD4$^+$ T cells may play a critical role in combatting poxvirus infections of the skin.

Skin is the largest organ system of the body and serves as the critical physical barrier preventing pathogens and commensal microbes from infiltrating vulnerable tissues. The epidermis is the outermost layer of the skin that is directly exposed to the environment and is composed primarily of keratinocytes in various stages of differentiation. Self-renewing basal layer keratinocytes are attached to the basement membrane that separates the epidermis from the underlying dermis, and the subsequent differentiation and ultimate death of keratinocytes results in the formation of the outermost keratin-rich cornified layer, the stratum corneum.[23] Besides providing this tight physical barrier between "self" and the environment, there is additional experimental evidence that keratinocytes may play important roles in the coordination of immune responses within the skin. Keratinocytes express a variety of pattern recognition receptors and thus have the capacity to detect pathogen invasion and subsequently promote inflammatory responses through the production of a number of different cytokines and chemokines.[24] Alternatively, keratinocytes also promote immune tolerance by producing thymic stromal lymphopoietin (TSLP), which locally activates regulatory CD4$^+$ T cells, and express $\alpha_v\beta_6$ and $\alpha_v\beta_8$ integrins that are necessary to activate transforming growth factor β (TGF-β) within the epidermis.[25,26] Keratinocytes also become infected by several types of viruses including poxviruses,[27] but whether keratinocytes are critical targets of anti-viral adaptive immunity to prevent viral infection of the skin remains to be fully determined.

Here, we report that antigen-specific memory CD4$^+$ T cells that form following immunization are sufficient to provide complete and broad protection against poxvirus infections of the skin. Trafficking of memory CD4$^+$ T cells into the skin was restricted to Th1-T$_{EM}$ T cells that synthesized core 2 O-glycans on PSGL-1, and memory CD4$^+$ T cells had to enter the skin to provide immunity against the viral infection. Within the skin microenvironment, memory CD4$^+$ T cells rapidly produced IFNγ in an antigen-specific manner, causing global changes in gene expression to promote anti-viral immunity. Keratinocytes increased antigen presentation pathways during viral skin infection in an IFNγ-dependent manner, and IFNγ receptor (IFNγR) signaling and MHC class II expression by keratinocytes was necessary for memory CD4$^+$ T cells to fully protect the skin from poxvirus infection. Notably, vaccination with MVA failed to generate Th1 memory CD4$^+$ T cells that could protect against zoonotic poxvirus infection. Overall, these findings reveal a currently underappreciated role for memory CD4$^+$ T cells in coordinating anti-viral responses and highlight the importance of keratinocytes being critical targets of CD4$^+$ T cell-mediated cellular immunity to limit poxvirus replication and spread within the skin.

RESULTS

Memory CD4$^+$ T cells protect the skin from poxvirus infection

Zoonotic poxviruses (e.g., CPXV and mpox) are spread primarily by direct contact with infected skin lesions. To test if and how effectively traditional VacV immunization would protect the skin from zoonotic poxvirus infection, we immunized mice with tk^- VacV by skin scarification (which is less pathogenic than WT VacV[28]) and then infected distal skin with CPXV 30 days later (Figure 1A). To first determine whether VacV immunization generated memory CD8$^+$ and/or CD4$^+$ T cells, we used previously identified MHC class I and class II epitopes highly conserved across *Orthopoxvirus* species to stimulate splenocytes and analyzed IFNγ/tumor necrosis factor α (TNF-α) production by CD8$^+$ and CD4$^+$ T cells.[29,30] Antigen-specific memory CD8$^+$ and CD4$^+$ T cells were detectable in VacV-immune mice prior to infection, and both underwent secondary expansion following CPXV infection of the skin (Figures 1B, 1C, S1A, and S1B). CPXV replication was robust in the skin of naive animals and caused considerable pathology, whereas VacV immunization largely prevented and cleared the viral infection, and immunized mice did not develop the necrotic skin lesions observed in the naive controls (Figures 1D and S1C). These data demonstrate that VacV immunization generates both memory CD8$^+$ and CD4$^+$ T cells and provides significant protection against zoonotic poxvirus infection of the skin.

Successful vaccinations typically result in the generation of both cellular and humoral immunity, but the relative contributions of antibodies and memory T cells in mediating protection against poxvirus infections of the skin remain unresolved. Because we observed that both memory CD8$^+$ and CD4$^+$ T cells were generated by VacV immunization, we next asked whether cytotoxic or helper T cells would be necessary to protect VacV-immunized animals from poxvirus skin infections (Figure 1E). Depletion of CD4$^+$ T cells caused a significant loss of protection against CPXV skin infection, whereas immunized mice depleted of CD8$^+$ T cells were still fully protected (Figure 1F). Notably, depletion of both CD4$^+$ and CD8$^+$ T cells did not cause any additional loss of protection compared with depleting only the CD4$^+$ T cells, suggesting that memory CD8$^+$ T cells play little role in protecting the skin from zoonotic poxvirus infections. Depletion of CD8$^+$ T cells also did not result in any loss of protection against wild-type (WT) VacV Western Reserve (VacV-WR) skin infection, whereas a modest, albeit significant, level of protection was lost when CD4$^+$ T cells were depleted (Figure 1G). However, when both CD8$^+$ and CD4$^+$ T cells were depleted prior to infection with VacV-WR, viral load was ~1,000–5,000× higher compared with immune, control-treated animals. Thus, these data demonstrate that both CD8$^+$ and CD4$^+$ memory T cells protect against VacV, but only memory CD4$^+$ T cells protect the skin from CPXV infection.

Prior studies have found that CPXV can limit antigen presentation to CD8$^+$ T cells by preventing surface expression of MHC class I on infected cells.[18] In CPXV and mpox, this gene is encoded by *CPXV203* and *B10R*, respectively, and an analysis of whole-genome sequences of patients with mpox during the 2022 outbreak demonstrates the high conservation of this gene among the mpox viruses that are spreading (Figures S2A and S2B). The ortholog of these genes in VacV, *B9R*, has acquired a frameshift mutation resulting in a truncated version of the protein, which could explain why memory CD8$^+$ T cells can protect the skin from VacV-WR but not CPXV. To directly test whether inhibition of MHC class I expression was the mechanism that allowed CPXV to successfully evade memory CD8$^+$ T cells,
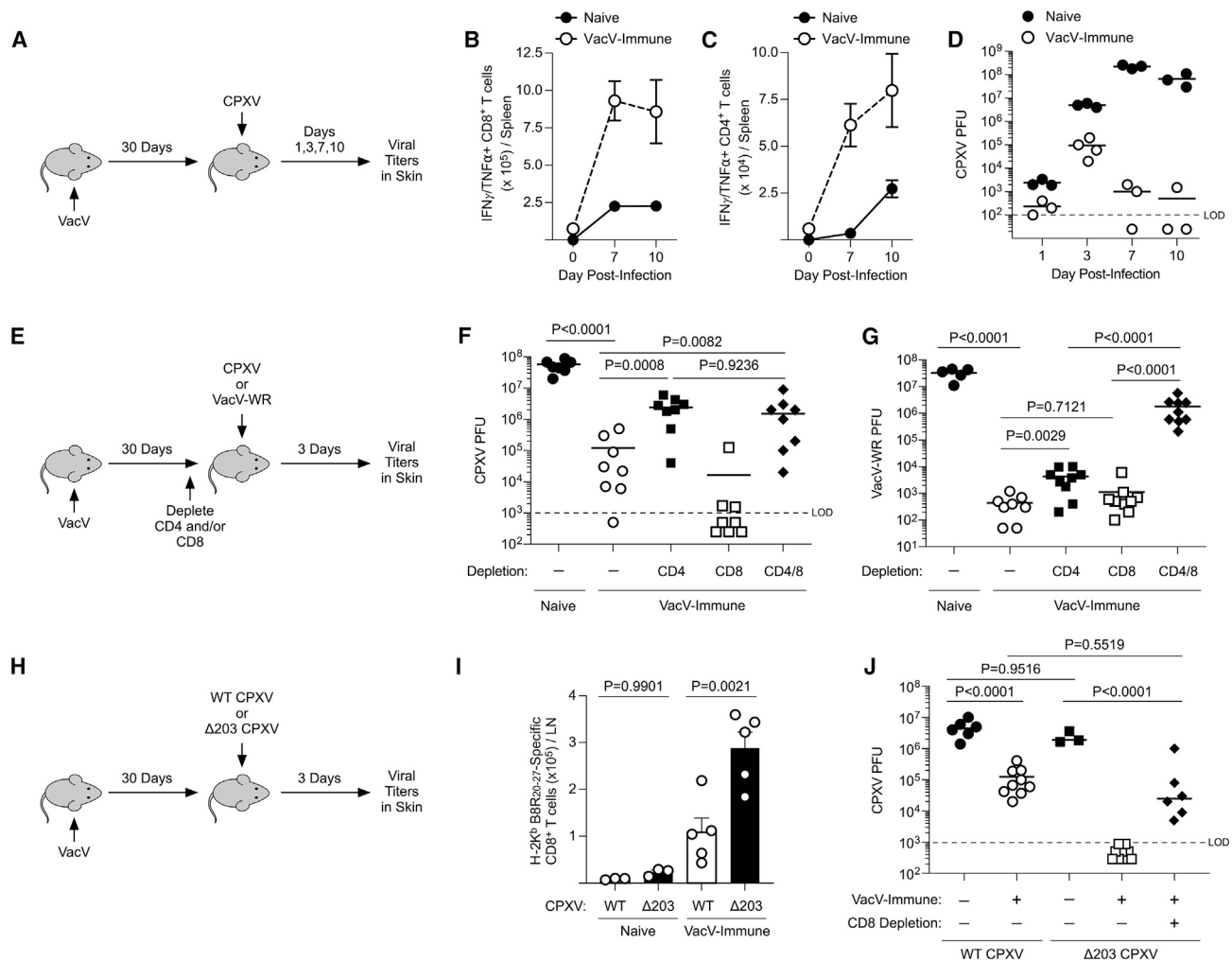
Figure 1. Memory CD4+ T cells protect the skin from zoonotic poxvirus infection

(A) Experimental design for (B)–(D).

(B) Number of CD8+ T cells producing IFNγ/TNF-α from the spleen following stimulation with B8R$_{20-27}$ peptide.

(C) Number of CD4+ T cells producing IFNγ/TNF-α from the spleen following stimulation with I1L$_{7-21}$, L4R$_{173-187}$, and H3L$_{269-283}$ peptides.

(D) CPXV PFU from skin on the indicated day post-infection.

(E) Experimental design for (F) and (G).

(F) CPXV PFU from skin on day 3 post-infection.

(G) VacV-WR PFU from skin on day 3 post-infection.

(H) Experimental design for (I) and (J).

(I) Number of B8R$_{20-27}$ specific CD8+ T cells in the draining lymph node on day 3 post-infection.

(J) CPXV or Δ203CPXV PFU from skin on day 3 post-infection.

Data are mean ± SD and are representative or combined from 2 or more independent experiments. Dashed lines indicate limit of detection (LOD).

See also Figure S1 and S2.

we infected VacV-immunized mice or naive controls with WT CPXV or Δ203CPXV (Figure 1H). Consistent with this hypothesis, memory CD8+ T cell secondary expansion was greater in the draining lymph node of mice infected with Δ203CPXV than those infected with the WT virus (Figures 1I and S2C). VacV-immune mice were completely protected from Δ203CPXV compared with WT CPXV infection, whereas both viruses replicated similarly in naive controls (Figure 1J). Importantly, depletion of CD8+ T cells prior to infection caused a loss of protection against Δ203CPXV, demonstrating that the virus was susceptible to be-

ing identified and eliminated by memory CD8+ T cells. Altogether, these data demonstrate that zoonotic poxviruses can successfully evade memory CD8+ T cells and highlight the critical role for memory CD4+ T cells in protecting the skin from poxvirus infections.

Because we observed that memory CD4+ T cells were required to protect the skin from a zoonotic poxvirus, we next asked whether antigen-specific memory CD4+ T cells would also be sufficient to protect against a poxvirus skin infection. To test this, we immunized mice with lymphocytic choriomeningitis virus
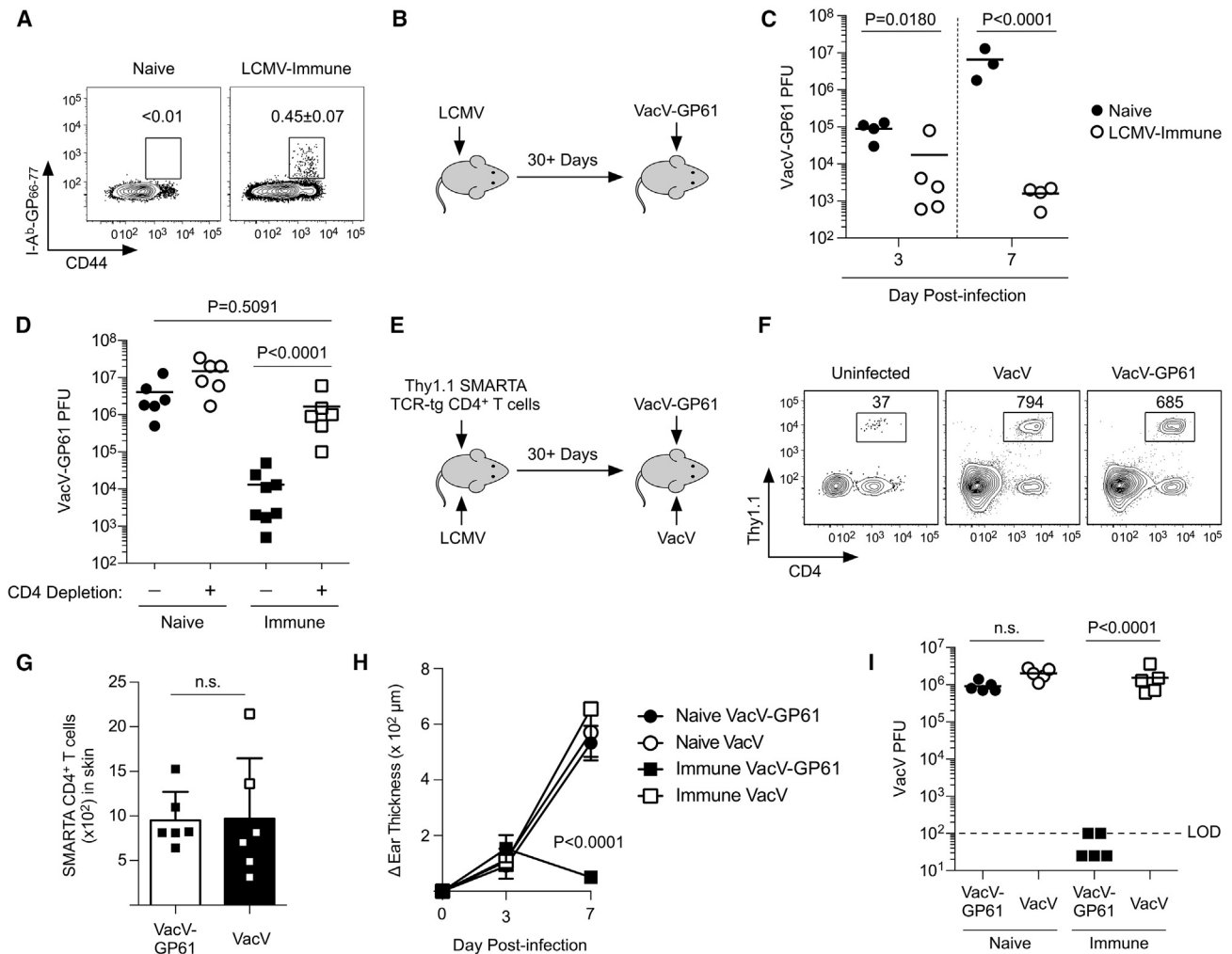
Figure 2. Memory CD4⁺ T cells are sufficient to protect the skin from poxvirus infection

(A) GP$_{61-80}$-specific CD4⁺ T cells were identified 40 days after LCMV infection.

(B) Experimental design for (C) and (D).

(C) VacV-GP61 PFU from skin on days 3 and 7 post-infection.

(D) Same as (C) except mice received CD4-depleting antibodies or control immunoglobulin G (IgG) prior to VacV-GP61 infection. Viral titers were measured on day 7 post-infection.

(E) Experimental design for (F)–(I).

(F) Trafficking of memory SMARTA CD4⁺ T cells into the skin on day 3 post-infection.

(G) Quantification of (F).

(H) Tissue swelling was measured on the indicated day post-infection.

(I) Same mice as (H) except viral titers were measured on day 7 post-infection.

Data are mean ± SD and are representative of 2 or more independent experiments. Dashed line indicates LOD.

See also Figure S3.

(LCMV) to generate memory CD4⁺ T cells specific for the I-A^b-restricted, immunodominant epitope from the LCMV glycoprotein, amino acids 61–80 (GP61). Following LCMV infection, GP61-specific T cells readily expanded (identified using GP$_{66-77}$ loaded I-A^b tetramer), accounting for over 5% of all CD4⁺ T cells on day 7 post-infection (Figures S3A and S3B). GP61-specific CD4⁺ T cells continued to persist following contraction, and using the markers Ly6C and CCR7 to identify T$_{EM}$ and T$_{CM}$ T cells, respectively,[13] both populations were represented at

day 40 post-infection (Figures 2A, S3C, and S3D). LCMV-immune mice or naive controls were then challenged with VacV expressing MHC class II-targeted GP$_{61-80}$ (VacV-GP61)[31] (Figure 2B), as only memory CD4⁺ T cells from LCMV-immune mice, and not CD8⁺ T cells, produce IFNγ following stimulation with this peptide (Figure S3E). LCMV-immune mice were protected from VacV-GP61 skin infection, and virus was essentially cleared by day 7 post-infection (Figure 2C). Depletion of CD4⁺ T cells resulted in a complete loss of protection (Figure 2D),

whereas depletion of CD8$^+$ T cells had no effect (Figure S3F), demonstrating that antigen-specific memory CD4$^+$ T cells were solely responsible for eliminating virus and that "bystander" activation of memory CD8$^+$ T cells does not significantly limit poxvirus replication in the skin.

Finally, to determine whether the protective immunity provided by memory CD4$^+$ T cells was antigen and/or tissue specific, we transferred SMARTA T cell receptor (TCR)-transgenic CD4$^+$ T cells into B6 mice and infected them with LCMV to generate a readily trackable population of GP61-specific CD4$^+$ T cells. LCMV-immune mice were then infected with VacV on the right ear skin and VacV-GP61 on the left (Figure 2E). Memory SMARTA CD4$^+$ T cells trafficked equally to both VacV- and VacV-GP61-infected skin (Figures 2F and 2G), demonstrating that like memory CD8$^+$ T cells,[32] memory CD4$^+$ T cells traffic into VacV-infected skin in an antigen-independent manner. GP61-specific memory CD4$^+$ T cells in LCMV-immune animals limited tissue pathology (swelling) and provided complete protection against the VacV-GP61 infection (Figures 2H and 2I) but provided no protection against the VacV infection. Overall, these data demonstrate that antigen-specific memory CD4$^+$ T cells provide significant protective immunity against poxvirus skin infection in both a tissue- and antigen-specific manner.

Th1 effector memory CD4$^+$ T cells synthesize core 2 O-glycans and traffic into the skin to protect against poxvirus infection

As shown previously, memory CD4$^+$ T cells differentiate into Ly6C$^+$ T$_{EM}$ and CCR7$^+$ T$_{CM}$ following acute viral infection (Figure S3). To determine whether all memory CD4$^+$ T cells could traffic into the skin or if restricted to certain subsets, we challenged LCMV-immune mice with VacV and analyzed which memory CD4$^+$ T cells trafficked into the skin. The memory CD4$^+$ T cells that infiltrated the skin were predominately Ly6C$^+$ T$_{EM}$, whereas CCR7$^+$ T$_{CM}$ cells were essentially excluded (Figure 3A). Core 2 O-glycan synthesis is essential for the generation of functional ligands for the vascular adhesion molecules P- and E-selectin, which initiate non-lymphoid tissue extravasation.[33] Indeed, the Ly6C$^+$ memory CD4$^+$ T cells that trafficked into the skin following VacV infection also expressed core 2 O-glycans (identified using the monoclonal antibody 1B11) (Figures 3B and 3C). Thus, these data demonstrate that the Th1 memory CD4$^+$ T cells that traffic into the skin are Ly6C$^+$ T$_{EM}$ and synthesize core 2 O-glycans.

Ly6C$^+$ memory CD4$^+$ T cells expressed higher levels of PSGL-1 (Figure 3D), as well as more unsialylated core 1 O-glycans (identified by reactivity with the lectin peanut agglutinin [PNA]) (Figure 3E), which is necessary for core 2 O-glycan synthesis to occur.[34] Ly6C$^+$ T$_{EM}$ also expressed higher levels of the interleukin-2β (IL-2β) receptor (CD122) (Figure 3F), which we have previously shown to be critical for promoting IL-15-stimulated synthesis of core 2 O-glycan on T$_{CM}$ CD8$^+$ T cells.[32] In agreement with these findings, Ly6C$^+$ T$_{EM}$ bound to P- and E-selectin more than Ly6C$^-$ T cells, and administration of P-selectin and E-selectin blocking antibodies prevented the trafficking of memory CD4$^+$ T cells into the skin following VacV infection, resulting in a complete loss of protection (Figures 3G–3J). These data demonstrate that the capacity to synthesize ligands

for P- and E-selectin is critical for memory CD4$^+$ T cells to infiltrate VacV-infected skin to provide anti-viral immunity.

PSGL-1 is required for Th1 effector memory CD4$^+$ T cells to traffic into the skin during poxvirus infection

Once decorated with specialized core 2 O-linked glycans, PSGL-1 can function as both a P- and E-selectin ligand in some cell types.[35] Because our previous analyses demonstrated that Ly6C$^+$ T$_{EM}$ CD4$^+$ T cells synthesized core 2 O-glycans, we next investigated whether PSGL-1 was functioning as the major ligand for either P- and/or E-selectin and whether PSGL-1 was required for memory CD4$^+$ T cells to traffic into the skin. At day 40 post-infection with LCMV, the frequencies and differentiation of Ly6C$^+$ T$_{EM}$ and CCR7$^+$ T$_{CM}$ CD4$^+$ T cells were largely similar in both WT and Selplg$^{-/-}$ animals (Figures S4A–S4D), but Selplg$^{-/-}$ memory CD4$^+$ T cells were limited in their ability to bind to both P- and E-selectin (Figures S4E–S4G). Following VacV skin infection, both total and GP61-specific memory CD4$^+$ T cells that trafficked into VacV-infected skin were reduced in Selplg$^{-/-}$ animals, even though there were more GP61-specific memory CD4$^+$ T cells in the spleen (Figures S4H–S4J). Accordingly, memory CD4$^+$ T cell-mediated protective immunity against VacV skin infection was significantly compromised in Selplg$^{-/-}$ mice (Figure S4K). These data show that PSGL-1 is an essential ligand for both P- and E-selectin on Th1 T$_{EM}$ CD4$^+$ T cells and is critical for trafficking into the skin during a poxvirus infection.

Antigen-specific memory CD4$^+$ T cells rapidly produce IFNγ and induce a highly inflammatory, anti-viral state in the skin microenvironment during poxvirus infection

Because our data showed that memory CD4$^+$ T cells needed to infiltrate VacV-infected skin to provide protective immunity, we next sought to define the changes in gene expression that antigen-specific memory CD4$^+$ T cells were causing in the skin microenvironment. We infected LCMV-immune mice with VacV-GP61 on the left ear skin and VacV on the right and analyzed changes in gene expression by genome-wide RNA sequencing (Figure 4A). This approach allowed us to evaluate specifically the effect that antigen-specific memory CD4$^+$ T cells were having on the skin microenvironment following poxvirus infection, as GP61-specific memory CD4$^+$ T cells would also infiltrate VacV-infected skin on the same animal but not provide any level of protection (Figure 2I). Both principal-component analysis (PCA) and hierarchical clustering demonstrated striking distinctions in global gene expression between the experimental groups, and 1,912 genes became significantly (false discovery rate [FDR] < 0.05) upregulated with fold change >2 in skin where protection was being provided by memory CD4$^+$ T cells compared with the control, VacV-infected skin on the same animal (Figures 4B and 4C). These included a number of pro-inflammatory cytokines (Ifng, Il1a, Il1b, and Il12a) and targets of IFNγ signaling (Arg1, Nos2, Itim1, and Cxcl9), as well as genes critical for antigen presentation (B2m, Tap1, Tap2, CD74) (Figure S5A).

Gene Ontology analysis revealed enrichments of a number of biological processes including "immune and defense responses," "cytokine production," and "lymphocyte activation,"
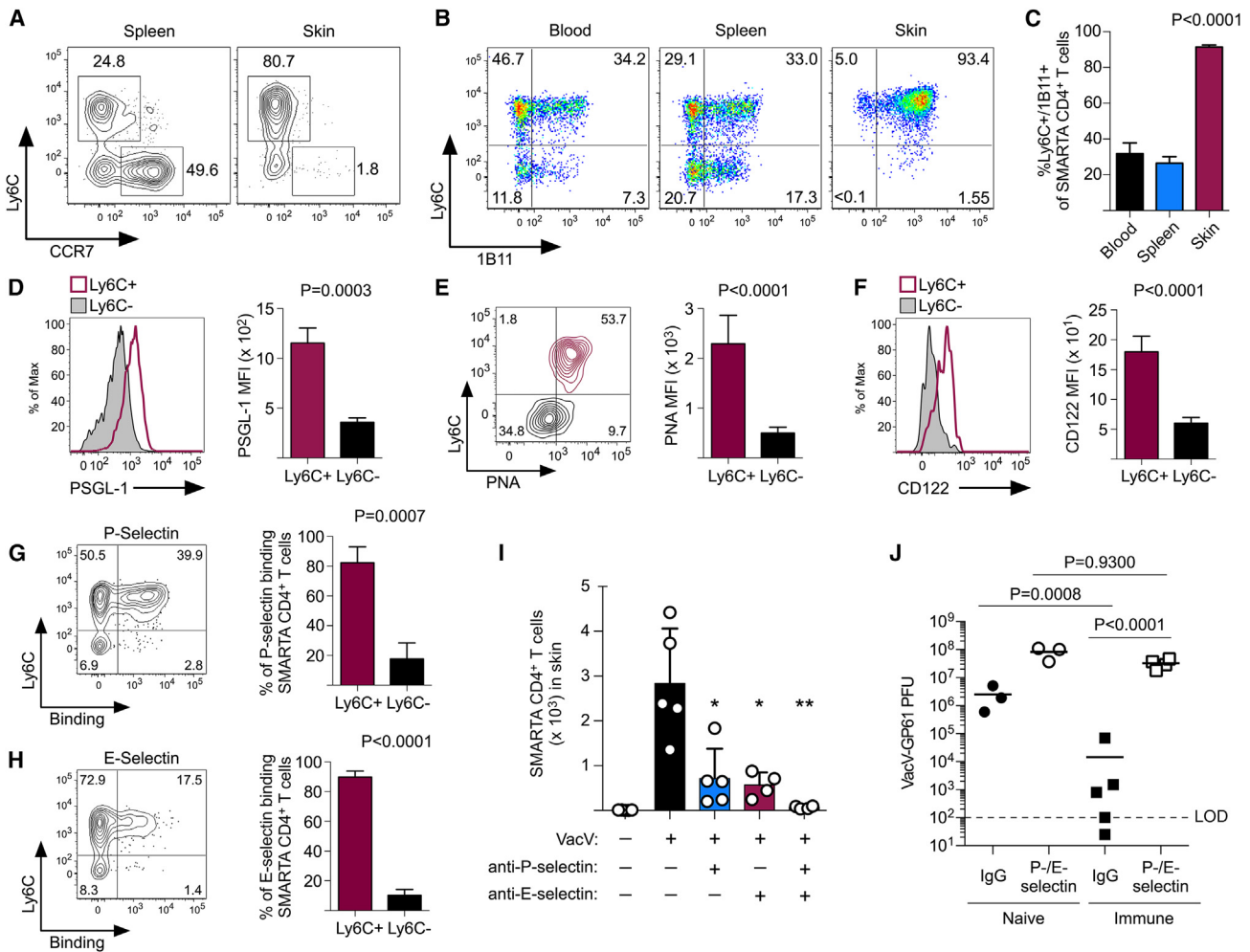
Figure 3. Ly6C+ T_EM CD4+ T cells synthesize core 2 O-glycans and traffic into the skin during poxvirus infection
(A) LCMV-immune mice were infected with VacV, and expression of Ly6C and CCR7 was analyzed on SMARTA CD4+ T cells on day 3 post-infection.
(B) Same as (A) except expression of glycosylated CD43 (clone 1B11) and Ly6C was analyzed.
(C) Quantification of (B).
(D) PSGL-1 expression by Ly6C+ and Ly6C− memory SMARTA CD4+ T cells.
(E) Unsialylated core 1 O-glycans expression measured using PNA reactivity by Ly6C+ and Ly6C− memory SMARTA CD4+ T cells.
(F) CD122 expression by Ly6C+ and Ly6C− memory SMARTA CD4+ T cells.
(G and H) Quantification of Ly6C expression on memory SMARTA CD4+ T cells that bind to (G) P-selectin or (H) E-selectin.
(I) LCMV-immune mice with SMARTA CD4+ T cells were infected with VacV on the left ear skin and treated with blocking antibodies as indicated. Trafficking of memory SMARTA CD4+ T cells into the skin was quantified on day 3 post-infection.
(J) LCMV-immune mice or naive controls were infected with VacV-GP61 and administered control IgG or P-/E-selectin-blocking antibodies. Viral titers were measured on day 7 post-infection.
Data are mean ± SD and are representative of 2 or more independent experiments. Dashed line indicates LOD.*p < 0.005, **p < 0.001.

suggesting global changes in gene expression that would promote anti-viral immunity (Figure S5B). Gene set enrichment analysis (GSEA) also identified that IFNγ signaling pathways were highly enriched in VacV-GP61-infected skin compared with VacV-infected skin (Figures 4D and 4E). Finally, to confirm that antigen-specific memory CD4+ T cells were responsible, we compared gene expression from VacV-GP61- and VacV-infected skin of naive and LCMV-immune animals. Expressions of *Ifng*, *Cxcl9*, *Il1a*, *Arg1*, *Gbp10*, and *Gbp2* were all upregulated specifically in VacV-GP61-infected skin compared with VacV-in-

fected skin of immune animals but not in naive controls (Figure S5C). Thus, these data demonstrate that antigen-specific memory CD4+ T cells are sufficient to cause rapid and profound changes in gene expression within the skin microenvironment that limits viral spread and/or replication.

Because our data suggested that IFNγ signaling was significantly enriched in skin where memory CD4+ T cells were providing protective immunity, we next asked whether memory CD4+ T cells produced this cytokine in an antigen-specific manner within the skin microenvironment. We transferred IFNγ-YFP
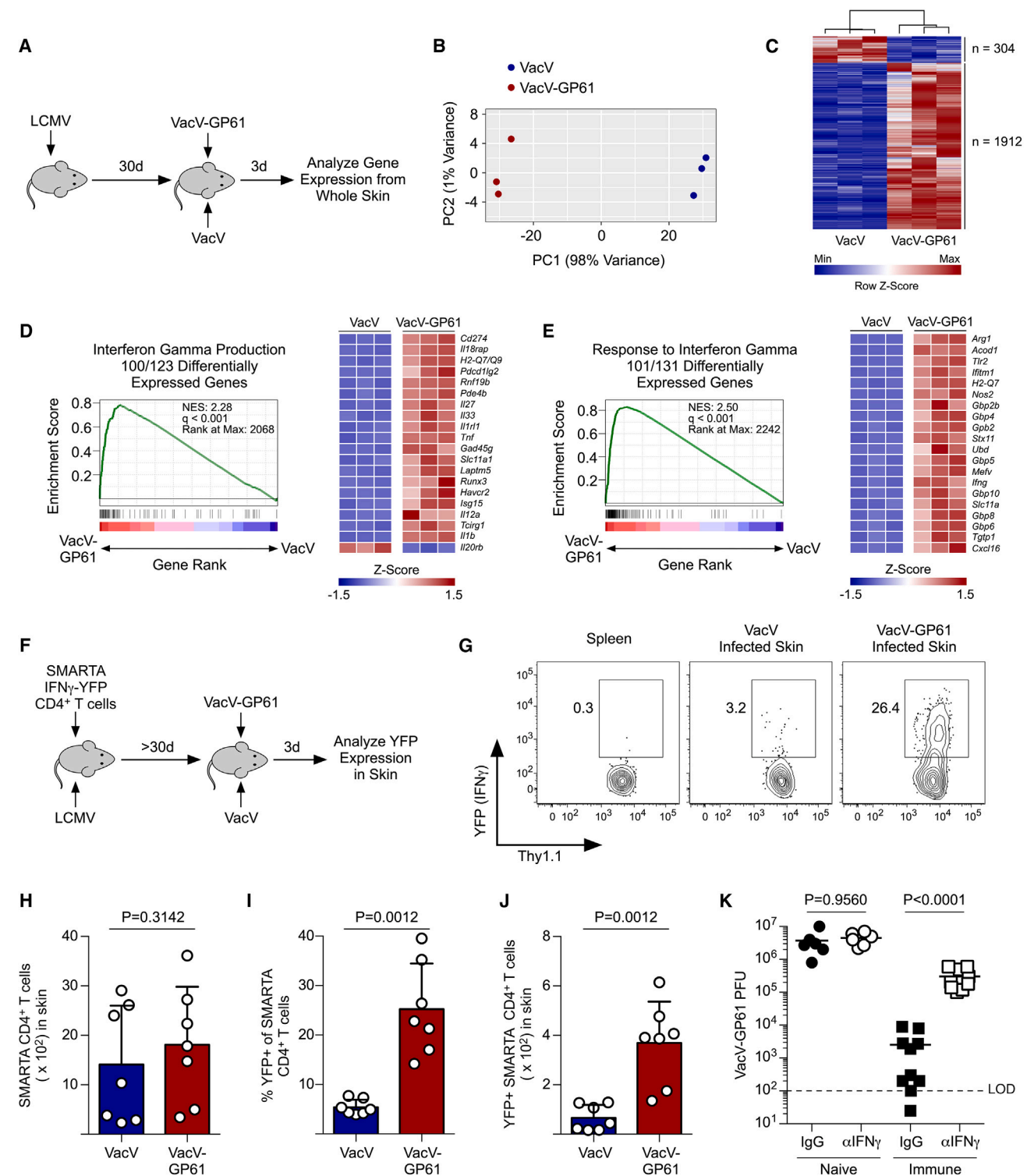
Figure 4. Antigen-specific memory CD4+ T cells rapidly produce IFNγ and promote anti-viral immunity against poxvirus skin infection

(A) Experimental design for gene expression analysis from whole skin.

(B) Principal-component analysis (PCA) of gene expression profiles from (A).

(C) Heatmap of differentially expressed genes from (A).

(D) GSEA plot and *Z* score heatmap of the top 20 most differentially expressed genes in GO term "interferon gamma production."

(E) Same as (D) except for GO term "response to interferon gamma."

SMARTA CD4$^+$ T cells into naive B6 mice followed by infection with LCMV. At >30 days after LCMV infection, we infected mice on the left ear skin with VacV-GP61 and VacV on the right ear skin and analyzed expression of IFNγ (YFP) directly *ex vivo* on day 3 post-infection (Figure 4F). Memory CD4$^+$ T cells expressed IFNγ in skin infected with VacV-GP61 but not in the spleen or skin infected with VacV, despite trafficking into both sites of viral infection equally (Figures 4G–4J). Neutralization of IFNγ during VacV-GP61 infection reduced the protective effect of memory CD4$^+$ T cells (Figure 4K), suggesting that production of IFNγ by Th1 T$_{EM}$ CD4$^+$ T cells was necessary for protecting against the viral skin infection. Of note, these data also suggest that only a few hundred IFNγ-producing memory CD4$^+$ T cells are required to provide complete protection against VacV skin infection.

Keratinocytes are highly sensitive targets of IFNγ signaling and express MHC class II during poxvirus skin infection

Keratinocytes are the major cell type of the epidermis, provide the critical environmental barrier to protect vulnerable tissues against invasion by microbial pathogens, and have been reported to become infected with VacV.[36] To quantify the extent to which keratinocytes are targeted by poxviruses, we infected the skin with VacV expressing GFP (VacV-GFP) and quantified GFP+ cells on day 3 post-infection. We utilized a previously described gating strategy to identify keratinocytes in the epidermis by flow cytometry (Figure S6A), where CD45− cells from the epidermis that express Sca-1 represent keratinocytes from either the interfollicular epidermis or infundibulum, whereas cells that do not express Sca-1 are largely from the hair follicle.[37] Almost 1% of all keratinocytes became GFP+, and ∼90% of the total GFP+ cells in the epidermis following VacV-GFP infection were CD45−/Sca-1+ compared with CD45−/Sca-1− cells and CD45+ hematopoietic cells (Figures 5A and 5B). This finding demonstrates that keratinocytes are highly susceptible to and are the major cellular target of poxvirus infection of the epidermis.

Because our transcriptional profile demonstrated that IFNγ signaling and antigen presentation were both upregulated in the skin by antigen-specific memory CD4$^+$ T cells during viral infection, we next determined whether keratinocytes dynamically regulated antigen-presentation pathways during a primary VacV infection. Expression of both MHC class I and class II by Sca-1+ keratinocytes in uninfected skin was relatively low or absent, respectively (Figure S6A). However, by day 7 post-VacV skin infection, essentially all keratinocytes expressed MHC class I, and ∼50% also expressed MHC class II (Figure 5C). This response by keratinocytes during VacV infection was both cell type- and tissue-specific, as MHC expression was not increased on Sca-1− cells of the hair fol-

licle or on keratinocytes from distal, uninfected skin. Interestingly, whereas MHC class II was transiently expressed by keratinocytes during viral infection and returned to baseline levels, MHC class I expression remained high even following viral clearance (Figures 5D and 5E), which occurs approximately 15 days after infection.[38] $Stat1^{−/−}$ mice did not express either MHC class I or class II following VacV infection (Figures 5F and 5G), suggesting a prominent role for IFN signaling in causing enhanced antigen presentation by keratinocytes. Receptors for type I (*Ifnar*) or type III IFNs (*Ifnlr*) were not required for keratinocytes to express MHC class I or class II following VacV infection (Figure S6B and S6C), whereas neutralizing IFNγ significantly reduced both (Figures 5H and 5I). Thus, these data show that type II IFN, but not type I or III, is critical for keratinocytes to increase expression of both MHC class I and class II during poxvirus infection.

IFN-stimulated genes (ISGs) play diverse and broad roles in anti-viral immunity and become expressed downstream of all three IFN receptors in a unique, but also often overlapping, fashion.[39] Because we found that MHC class II expression by keratinocytes peaked on day 7 during a primary VacV infection and was dependent on IFNγ, we next sorted keratinocytes at this time point and analyzed the expression of several known ISGs. *Gbp2*, *Gbp10*, *Gbp5*, *Oasl2*, *Ifit3*, and *Isg15* all became highly expressed by keratinocytes during VacV skin infection, and neutralizing IFNγ prevented their expression (Figure 5J), suggesting that type II IFN, rather than type I or III IFN, may be the primary IFN that acts on keratinocytes to promote anti-viral immunity. Overall, these data highlight that keratinocytes are highly sensitive targets of IFNγ signaling and may become critical targets of the cellular adaptive immune system to provide anti-viral immunity in the skin.

Keratinocytes require IFNγR signaling and MHC class II for memory CD4$^+$ T cells to protect the skin from poxvirus infection

Because our data demonstrated that keratinocytes were infected with VacV and were highly sensitive to the action of IFNγ, we next asked whether IFNγ signaling by keratinocytes would be required for memory CD4$^+$ T cells to protect the skin from poxvirus infection. To target deletion of the IFNγR specifically on keratinocytes, we generated mice with a floxed version of the IFNγR1 gene (*Ifngr1*$^{fl/fl}$) that were then crossed to mice expressing Cre recombinase driven by the cytokeratin 14 promoter (K14-Cre). By comparing *Ifngr1*$^{fl/fl}$ K14-Cre(−) with K14-Cre(+) mice, expression of IFNγR1 could be readily detected and eliminated on Sca1+ keratinocytes of the interfollicular epidermis and infundibulum (Figures 6A–6C). IFNγR1 expression was not detected on Sca-1−/CD34+ cells of the hair follicle bulge, and,

(F) Experimental design for (G)–(J).
(G) IFNγ expression (YFP) was analyzed on day 3 post-infection.
(H) Total number of SMARTA CD4$^+$ T cells in skin.
(I) Percentage of YFP+ SMARTA CD4$^+$ T cells from skin.
(J) Number of YFP+ SMARTA CD4$^+$ T cells in skin.
(K) Naive or LCMV-immune mice were infected with VacV-GP61 and given IFNγ neutralizing antibody or control IgG. Viral titers were measured on day 7 post infection.
Data are mean ± SD. (G)–(K) are representative of 2 independent experiments. Dashed line indicates LOD.
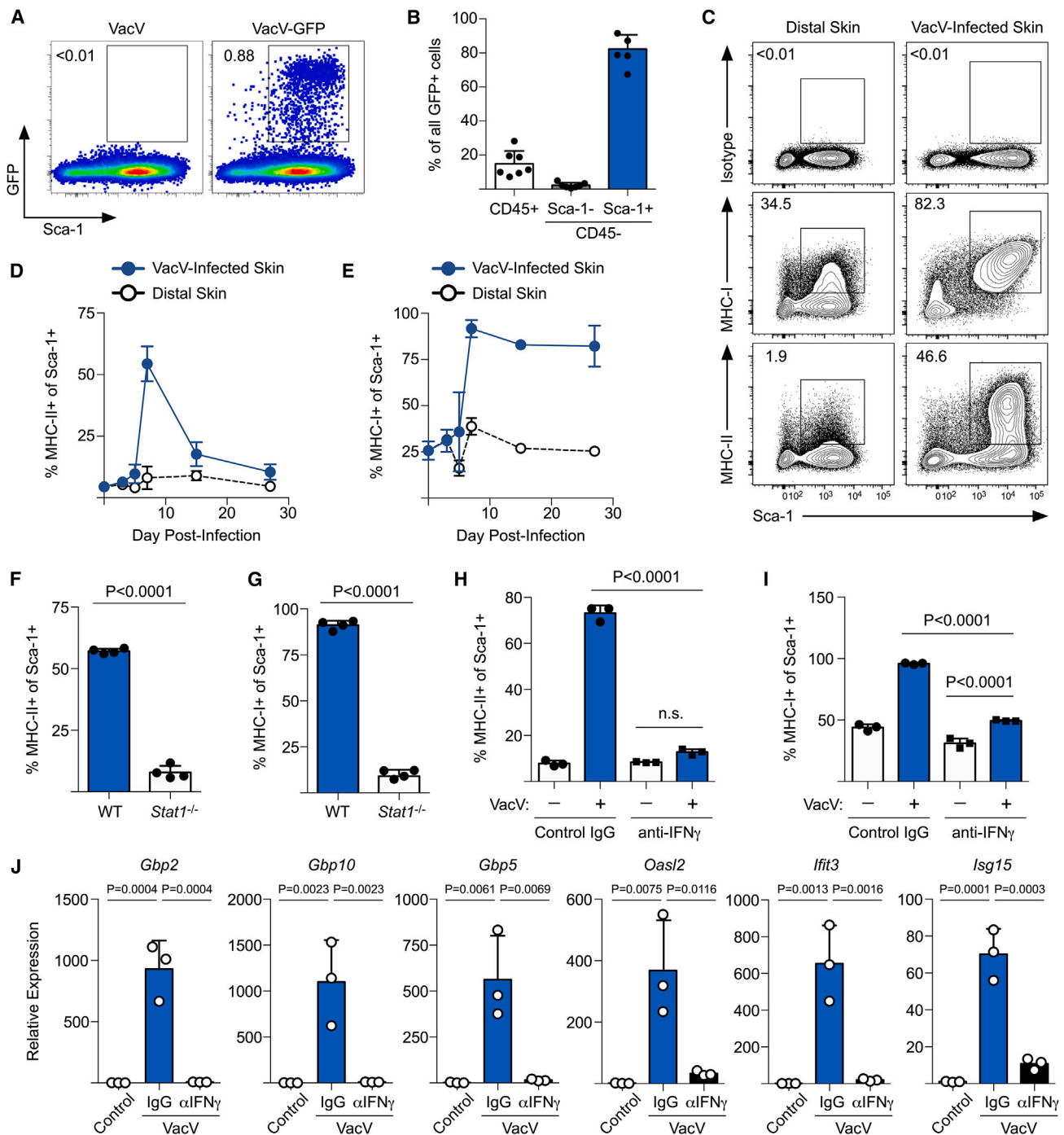See also Figure S5.

Figure 5. Keratinocytes express ISGs and upregulate MHC class I/II expression in an IFNγ-dependent manner during poxvirus infection

(A) Naive B6 mice were infected with VacV or VacV-GFP. GFP expression on CD45− cells was analyzed on day 3 post-infection.

(B) Distribution of GFP+ cells in the skin from (A).

(C) MHC class I and class II expression on CD45− cells from the epidermis of VacV-infected skin or uninfected, distal skin on day 7 post-infection.

(D and E) Quantification of (D) MHC class II and (E) class I expression by keratinocytes following VacV skin infection.

(F and G) Percentage of (F) MHC class II and (G) class I expression by keratinocytes following VacV infection of WT or $Stat1^{-/-}$ mice.

(H and I) Percentage of (H) MHC class II and (I) class I expression by keratinocytes following VacV infection of WT mice given control IgG or IFNγ neutralizing antibody.

(J) Sca-1+ keratinocytes were sorted on day 7 post-infection with VacV or from uninfected controls. Expression of the indicated ISG was quantified by qPCR.

Data are mean ± SD and are representative of 2 or more independent experiments.
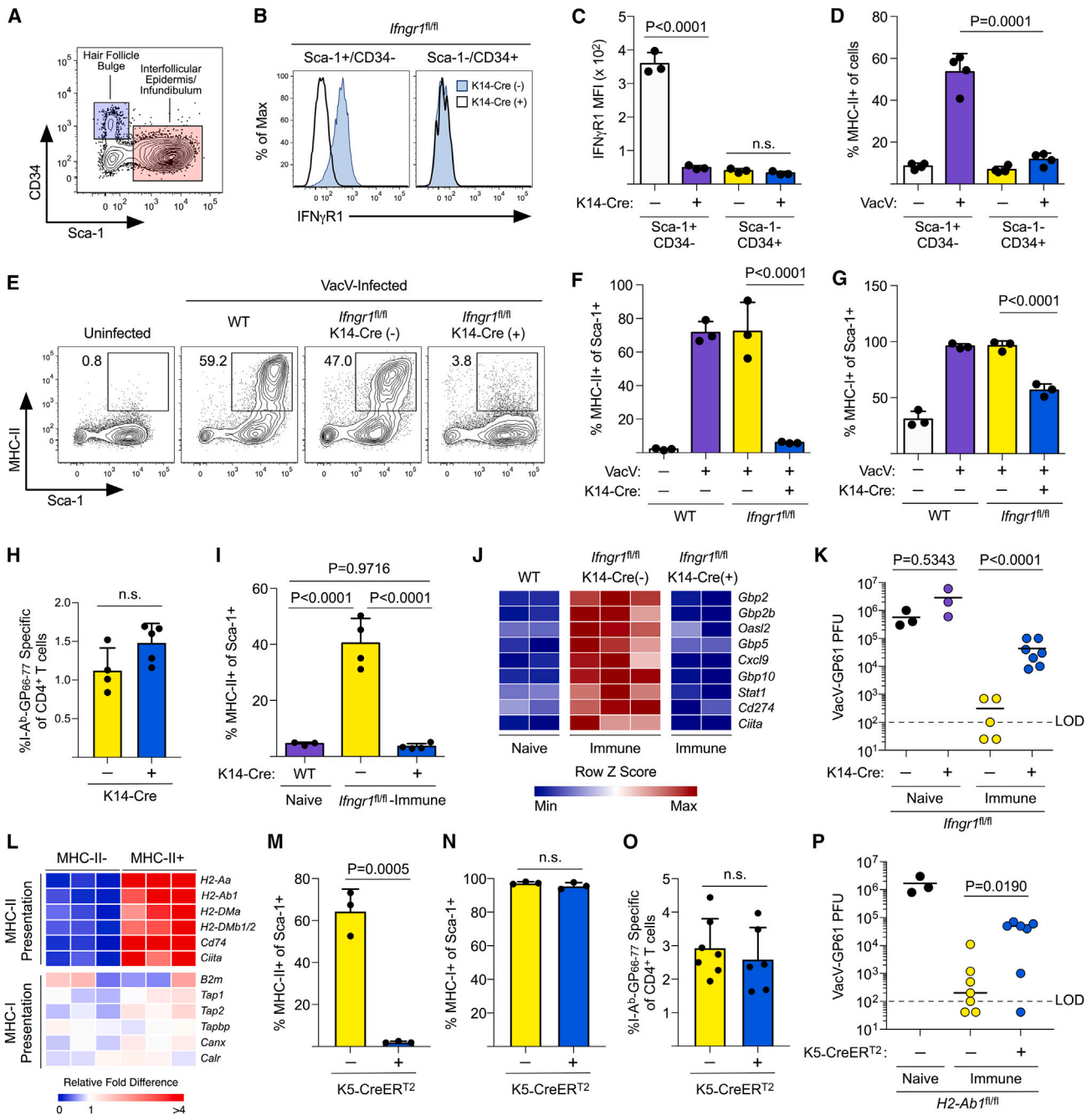
See also Figure S6.

Figure 6. IFNγR signaling and MHC class II expression by keratinocytes is required for memory CD4+ T cells to protect the skin from poxvirus infection

(A) Analysis of CD45− cells from skin. Cells of the hair follicle bulge (blue box) and keratinocytes of the interfollicular epidermis/infundibulum (pink box) are highlighted.

(B) IFNγR1 expression on skin cells shown in (A) from IFNγR1fl/fl K14-Cre(+) or IFNγR1fl/fl K14-Cre(−) mice.

(C) Quantification of IFNγR1 gMFI from (B).

(D) MHC class II expression from cell populations displayed in (A) on day 7 post-infection of WT mice with VacV.

(E) MHC class II expression of CD45− cells on day 7 post-infection with VacV.

(F) Quantification of (E).

(G) Quantification of MHC class I expression using same experimental design shown in (E).

(H) Frequencies of GP61-specific memory CD4+ T cells in *Ifngr1*fl/fl (K14-Cre+/−) mice on day 30 after LCMV infection.

(I) *Ifngr1*fl/fl (K14-Cre+/−) were immunized with LCMV and subsequently infected with VacV-GP61. MHC class II expression was analyzed on keratinocytes day 3 post-infection.

(legend continued on next page)

consistent with that finding, those cells did not express MHC class II after VacV infection (Figure 6D). IFNγR1-deficient keratinocytes failed to upregulate MHC class I and class II compared with both WT and *Ifngr1*fl/fl K14-Cre(−) mice during VacV infection (Figures 6E–6G). Thus, IFNγ signaling directly to keratinocytes is required for these cells to upregulate antigen-presentation pathways during poxvirus infection of the skin.

Having established that IFNγR signaling was sufficiently eliminated on *Ifngr1*fl/fl K14-Cre(+) keratinocytes, we next asked whether keratinocytes required expression of IFNγR1 for memory CD4+ T cells to protect the skin from poxvirus infection. We immunized *Ifngr1*fl/fl K14-Cre(+) and K14-Cre(−) animals with LCMV and, at day 30 post-infection, detected equal frequencies of GP61-specific memory CD4+ T cells between groups (Figure 6H). To determine whether IFNγ produced by memory CD4+ T cells was acting directly on keratinocytes, we infected LCMV-immune *Ifngr1*fl/f K14-Cre(+) and K14-Cre(−) animals with VacV-GP61 and analyzed expression of MHC class II on day 3 post-infection. Keratinocytes from *Ifngr1*fl/f K14-Cre(−) LCMV-immune animals expressed high levels of MHC class II compared with naive controls, but keratinocytes from *Ifngr1*fl/f K14-Cre(+) LCMV-immune animals did not (Figure 6I). Antigen-specific memory CD4+ T cells caused a number of ISGs to become rapidly expressed by keratinocytes early after infection, and this also required IFNγR1 (Figure 6J). Finally, IFNγ signaling to keratinocytes was critical for the anti-viral response, as there was a significant loss of protection against poxvirus infection of the skin when keratinocytes were unable to signal via the IFNγR (Figure 6K). Thus, these data demonstrate that immunity against poxvirus skin infection requires IFNγ produced by memory CD4+ T cells to signal directly to keratinocytes.

Our data showed that ~50% of keratinocytes expressed MHC class II following VacV infection, whereas MHC class I expression was essentially ubiquitous. Therefore, we next sorted MHC class II+ and MHC class II− keratinocytes and analyzed expression of a variety of genes necessary for presentation of peptides by MHC class II (Figure S6D). The master transcriptional regulator of MHC class II expression (*Ciita*), the MHC class II invariant chain (*Cd74*), and the non-classical MHC molecule H2-DM (*H2-Dma*, *H2-Dmb1/2*) were all more highly expressed in MHC class II+ keratinocytes compared with MHC class II− cells (Figure 6L). Consistent with our data showing that essentially all keratinocytes increase MHC class I expression, genes required for MHC class I presentation were similarly expressed between both subsets. To determine if MHC class II expression by keratinocytes was also required for memory CD4+ T cells to protect the skin from poxvirus infection, we generated *H2-Ab1*fl/fl mice crossed to cy-

tokeratin 5 (K5)-CreER[T2] to genetically disrupt MHC class II expression by keratinocytes in a temporal manner with tamoxifen. Tamoxifen treatment efficiently eliminated MHC class II expression by keratinocytes in *H2-Ab1*fl/fl K5-CreER[T2](+) mice, whereas MHC-I expression remained unchanged (Figures 6M and 6N). We next infected *H2-Ab1*fl/fl K5-CreER[T2](+) and K5-CreER[T2](−) animals with LCMV, treated them with tamoxifen after memory CD4+ T cells had formed, and then infected the skin with VacV-GP61. Following tamoxifen treatment and prior to infection with VacV-GP61, similar frequencies of GP61-specific memory CD4+ T cells were detected in both groups (Figure 6O), yet memory CD4+ T cells provided less protection when keratinocytes were unable to express MHC class II (Figure 6P). Collectively, these data show that IFNγR signaling and MHC class II expression by keratinocytes are critical for memory CD4+ T cells to fully protect the skin from poxvirus infection.

VacV vaccination provides greater protection against poxvirus infection of the skin than does MVA vaccination

MVA is a highly attenuated, replication-defective variant of VacV, but in a recent clinical trial, both vaccines were shown to generate similar levels of neutralizing antibodies.[11] To determine whether the two vaccines would also provide similar levels of immunity against poxvirus skin infections, we immunized mice with either VacV by skin scarification or a "prime-boost" regiment of MVA given two times subcutaneously (Figure 7A). Both vaccines caused expansion of antigen-specific CD8+ T cells and provided strong protection against a VacV-WR skin infection (Figures 7B–7D). Because the MVA vaccine generated antigen-specific memory CD8+ T cells and provided considerable protection against the VacV-WR infection, we next asked whether it would also protect against CPXV, since we also found that MVA immunization generated significantly fewer Ly6C+/CD44Hi memory CD4+ T cells than did the VacV vaccine (Figures 7E and 7F). Consistent with that observation, more poxvirus-specific CD4+ T cells producing IFNγ/TNF-α were detected in CPXV-infected mice vaccinated with VacV than mice given the MVA vaccination, whereas the number of antigen-specific CD8+ T cells producing cytokines was similar (Figures 7G, 7H, S7A, and S7B). Indeed, mice vaccinated with MVA were less protected from CPXV infection compared with the VacV vaccine and also developed necrotic skin lesions similar to naive controls (Figures 7I, 7J, and S7C). Thus, these data show that MVA vaccination does not generate significant levels of Th1 effector memory CD4+ T cells in mice and support our collective findings that memory CD4+ T cells are the key immune cell type responsible for protecting the skin from poxvirus infection.

(J) Same as (I) except keratinocytes were sort purified on day 4.5 post-infection. Expression of representative ISGs was quantified by qPCR.

(K) *Ifngr1*fl/fl (K14-Cre+/−) were immunized with LCMV and subsequently infected with VacV-GP61. VacV-GP61 PFU was quantified on day 7 post-infection.

(L) MHC class II+/− keratinocytes were sorted from the skin of naive mice infected with VacV on day 7 post-infection. MHC class I and class II antigen-presentation genes were quantified by qPCR.

(M and N) Naive *H2-Ab1*fl/fl (K5-CreERT2+/−) mice were supplied a tamoxifen diet as described in STAR Methods. (M) MHC class II or (N) class I expression by keratinocytes was analyzed on day 7 post-infection with VacV.

(O) *H2-Ab1*fl/fl (K5-CreERT2+/−) mice were infected with LCMV and subsequently placed on a tamoxifen diet as in (M) and (N). Frequencies of GP61-specific memory CD4+ T cells prior to infection with VacV-GP61.

(P) Same mice as (O). VacV-GP61 PFU from skin on day 7 post-infection.

Data are mean ± SD and are representative of 2 or more independent experiments. Dashed lines indicate LOD.
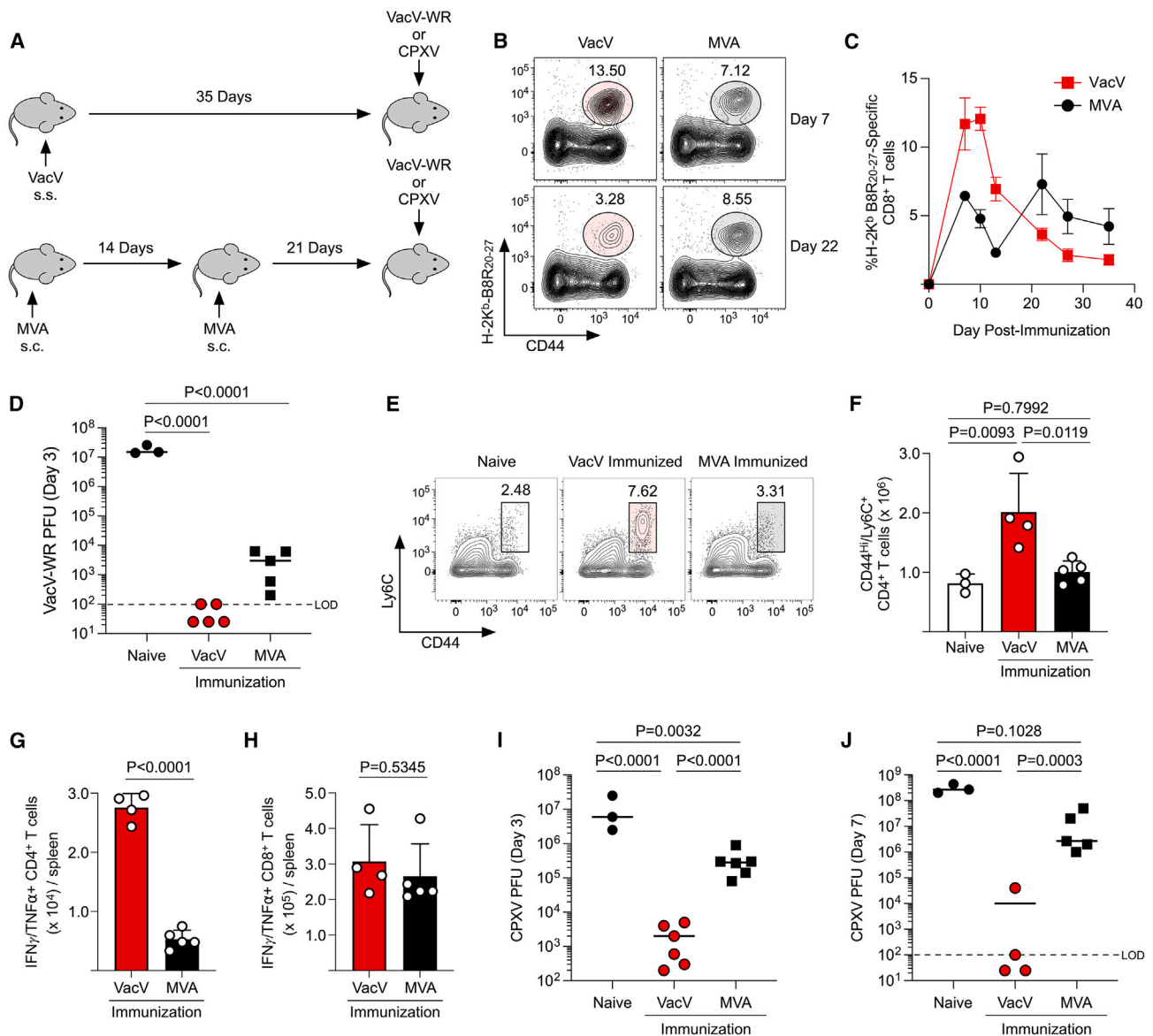
See also Figure S6.

Figure 7. MVA vaccination provides less protection against CPXV skin infection than does VacV vaccination

(A) Experimental design for (B)–(J).

(B) B8R$_{20-27}$-specific CD8$^+$ T cells were identified in the circulation on the indicated day post-infection.

(C) Longitudinal quantification of data shown in (B).

(D) VacV-WR PFU from skin on day 3 post-infection.

(E) Identification of Ly6C$^+$/CD44^{Hi} CD4$^+$ T cells in spleens of mice on day 7 post-infection with CPXV.

(F) Quantification of (E).

(G) Splenocytes were stimulated with I1L$_{7-21}$, L4R$_{173-187}$, and H3L$_{269-283}$ peptides on day 7 post-infection with CPXV. IFNγ-/TNF-α-producing CD4$^+$ T cells were quantified.

(H) Splenocytes were stimulated with B8R$_{20-27}$ peptide on day 7 post-infection with CPXV. IFNγ-/TNF-α-producing CD8$^+$ T cells were quantified.

(I and J) CPXV PFU from skin on (I) days 3 and (J) 7 post-infection.

Data are mean ± SD and are representative of 2 independent experiments. Dashed lines indicate LOD.

See also Figure S7.

DISCUSSION

CD4$^+$ T cells are critical for orchestrating adaptive immune responses by providing "help" to B cells, CD8$^+$ T cells, and macro-

phages, yet their ability to directly provide protection against different types of infections remains unresolved. There is clear evidence that CD4$^+$ T cells are responsible for protecting against several bacterial and parasitic infections that target macrophages

such as *Salmonella enterica* and *Leishmania major*.[40] In these instances, IFNγ produced by activated Th1 CD4^{+} T cells functions to increase expression of nitric oxide (NO) and reactive oxygen species (ROS) to mediate pathogen killing within the phagolysosome. Some infections may also lead to the development of cytotoxic helper CD4^{+} T cells that can directly kill MHC class II-expressing cells infected with pathogens.[41,42] How CD4^{+} T cells participate in anti-viral immunity remains less defined. In fact, in many instances, antigen-specific CD4^{+} T cells become pathogenic rather than protective during viral infections, causing significant morbidity and mortality.[43–47] This pathogenic effect is often enhanced in the absence of B cells or CD8^{+} T cells, suggesting a critical role for CD4^{+} T cell helper functions or an interplay between multiple arms of the adaptive immune system to provide protection against viral infections while also limiting severe immunopathology. In contrast to those findings, we demonstrate that antigen-specific Th1 T_{EM} CD4^{+} T cells are sufficient to provide protection and limit pathology during poxvirus infection of the skin.

The anti-viral activity of memory CD4^{+} T cells has been most widely studied during respiratory or systemic infections of mice, and the mechanisms of action, as well as the cell types involved, have yielded mixed results. During influenza infection, memory CD4^{+} T cells promote anti-viral activity through both cytolytic mechanisms and by accelerating antibody production.[48] Memory CD4^{+} T cells may also heighten innate inflammatory responses to respiratory viruses, as transferred Th1 or Th17 *in-vitro*-polarized CD4^{+} T cells prior to influenza infection cause the upregulation of pro-inflammatory cytokines and chemokines in the lung, but interestingly, that response does not require IFNγ or TNF-α.[49] CD4^{+} T cells that persist in the lung following influenza infection become activated following heterosubtypic influenza infection, and depletion of CD4^{+} T cells results in reduced protection against secondary challenge,[50] although more recent studies suggest that this protection may not be direct but rather through the subsequent action of "helped" CD8^{+} T cells or the local development of antibody-secreting B cells.[51,52] How memory CD4^{+} T cells coordinate anti-viral responses within the skin has not been thoroughly investigated. Interestingly, we have previously demonstrated that memory CD8^{+} T cells rapidly expressed granzyme B after infiltrating VacV-infected skin and required perforin to protect against poxvirus infection,[53] which contrasts our findings here demonstrating a critical role for memory CD4^{+} T cell-derived IFNγ to act directly on keratinocytes. Thus, CD4^{+} and CD8^{+} memory T cells may employ distinct, yet potentially synergistic, mechanisms to protect against viral skin infections.

Enzymatic synthesis of core 2 O-glycans is essential to provide the ligands for the vascular adhesion molecules P- and E-selectin.[33] Within T cells, O-linked glycan synthesis is a dynamic process that can be regulated through a variety of mechanisms, both antigen dependent and independent. Whereas core 2 O-glycan synthesis is most active in T_{CM} CD8^{+} T cells,[54] we found the opposite for Th1 memory CD4^{+} T cells, where core 2 O-glycan synthesis is largely a feature of the Ly6C^{+} T_{EM} population. In contrast to these highly mobilized Th1 T_{EM} CD4^{+} T cells, terminally differentiated KLRG1^{+} T_{EM} CD8^{+} T cells are limited in their ability to synthesize core 2 O-glycans and are

largely confined to the circulation.[54] Ly6C^{+} Th1 memory CD4^{+} T cells also express high levels of T-bet, and *in vitro* studies of CD4^{+} T cell differentiation suggest that T-bet may be critical for promoting core 2 O-glycan synthesis.[13,55] Alternatively, both T_{CM} CD8^{+} T cells and T_{EM} CD4^{+} T cells express high levels of the IL-2Rβ chain, suggesting that IL-15 signaling could also be a common mechanism that promotes the synthesis of core 2 O-linked glycans by both CD8^{+} and CD4^{+} memory T cells.[32]

Our study also found that keratinocytes are highly responsive to the action of IFNγ produced by memory CD4^{+} T cells during a viral skin infection and are the critical targets of IFNγ for preventing poxvirus infection of the epidermis. Previous studies have identified minor populations of MHC class II-expressing keratinocytes in mice and humans, and MHC class II expression is modestly upregulated (∼3%–5%) on keratinocytes following skin colonization with *S. epidermidis*.[56,57] However, that change in MHC class II expression required IL-22 and monocytes and not IFNγ, suggesting that different signaling pathways may be activated in keratinocytes during commensal bacterial colonization compared with a viral infection. In addition, MHC class II expression by keratinocytes was necessary for the development of Th1 CD4^{+} T cells in the skin, suggesting that antigen presentation by keratinocytes may regulate the T-helper differentiation profile or possibly the retention of Th1 CD4^{+} T cells locally.[56] In contrast to commensal bacterial colonization, our findings show that keratinocytes actively participate in the anti-viral adaptive immune response by being particularly responsive to the action of memory CD4^{+} T cell-derived IFNγ and upregulating antigen-presentation pathways to ultimately prevent viral replication.

In summary, our study shows that core 2 O-glycan-synthesizing memory CD4^{+} T cells exhibit robust anti-viral activity within the skin and reveal a previously uncharacterized mechanism linking the local activation of antigen-specific memory CD4^{+} T cells to the rapid delivery of IFNγ to keratinocytes, causing them to express ISGs and increase antigen presentation. Importantly, we also show that memory CD4^{+} T cells are the key immune cell type responsible for providing immunity against poxvirus infections of the skin, and it will be critical to determine whether poxvirus-specific Th1 effector memory CD4^{+} T cells form in those individuals currently receiving the MVA vaccine. Altogether, these results highlight an important relationship between virus-specific memory CD4^{+} T cells that traffic into the skin during infection to promote enhanced antigen presentation by keratinocytes while simultaneously limiting viral spread and/or replication, findings that are highly relevant for understanding the mechanisms connecting the protective cellular functions of the adaptive immune system to defined non-hematopoietic cell types that form environmental barrier tissues to ultimately provide host defense against viruses and other pathogens.

Limitations of the study

The experiments presented here were performed on laboratory mice, and it will need to be independently evaluated whether our findings translate to immune responses observed in humans following vaccination or zoonotic poxvirus skin infections. Critical outstanding questions directly related to this limitation

include: (1) do other zoonotic poxviruses such as mpox success-fully evade memory cytotoxic CD8$^+$ T cells in mice or humans? (2) Does IFNγR signaling prevent poxvirus infection and/or replication in human keratinocytes? (3) Do MVA vaccinations given to humans generate fewer poxvirus-specific Th1 effector memory CD4$^+$ T cells compared with traditional smallpox vaccinations with live VacV delivered by scarification of the skin?

STAR★METHODS

Detailed methods are provided in the online version of this paper and include the following:

- KEY RESOURCES TABLE
- RESOURCE AVAILABILITY
  - Lead contact
  - Materials availability
  - Data and code availability
- EXPERIMENTAL MODEL AND SUBJECT DETAILS
  - Mice
  - Viruses and infections
- METHOD DETAILS
  - Leukocyte isolation from skin
  - Isolation of epidermis for analysis of keratinocytes
  - Flow cytometry and cell sorting
  - *Ex vivo* peptide stimulation and intracellular stain
  - Antibodies and staining reagents
  - RNA sequencing and analysis
  - Quantitative PCR
- QUANTIFICATION AND STATISTICAL ANALYSIS
  - Statistical analyses

SUPPLEMENTAL INFORMATION

Supplemental information can be found online at https://doi.org/10.1016/j.celrep.2023.112407.

AUTHOR CONTRIBUTIONS

J.C.H. and J.C.N. designed and performed experiments, analyzed data, and wrote the manuscript. M.A., S.P.F., J.J.M., and T.J. Nappi performed experiments and analyzed data. Z.X. and S.L. assisted in the analysis of RNA sequencing data. T.J. Nice, J.B.S., and K.F. provided critical reagents.

DECLARATION OF INTERESTS

The authors declare no competing interests.

INCLUSION AND DIVERSITY

We support inclusive, diverse, and equitable conduct of research.

REFERENCES

1. Kozlov, M. (2022). How does monkeypox spread? What scientists know. Nature *608*, 655–656. https://doi.org/10.1038/d41586-022-02178-w.

2. McFadden, G. (2005). Poxvirus tropism. Nat. Rev. Microbiol. *3*, 201–213. https://doi.org/10.1038/nrmicro1099.

3. Hammarlund, E., Lewis, M.W., Hansen, S.G., Strelow, L.I., Nelson, J.A., Sexton, G.J., Hanifin, J.M., and Slifka, M.K. (2003). Duration of antiviral immunity after smallpox vaccination. Nat. Med. *9*, 1131–1137. https://doi.org/10.1038/nm917.

4. Parrino, J., and Graham, B.S. (2006). Smallpox vaccines: past, present, and future. J. Allergy Clin. Immunol. *118*, 1320–1326. https://doi.org/10.1016/j.jaci.2006.09.037.

5. World Health Organization (1980). The Global Eradication of Smallpox: Final Report of the Global Commission for the Certification of Smallpox Eradication (World Health Organization).

6. Wehrle, P.F. (1980). A reality in our time–certification of the global eradication of smallpox. J. Infect. Dis. *142*, 636–638. https://doi.org/10.1093/infdis/142.4.636.

7. Di Giulio, D.B., and Eckburg, P.B. (2004). Human monkeypox: an emerging zoonosis. Lancet Infect. Dis. *4*, 15–25. https://doi.org/10.1016/s1473-3099(03)00856-9.

8. 2022 mpox outbreak global map, https://www.cdc.gov/poxvirus/monkeypox/response/2022/world-map.html.

9. Alakunle, E.F., and Okeke, M.I. (2022). Monkeypox virus: a neglected zoonotic pathogen spreads globally. Nat. Rev. Microbiol. *20*, 507–508. https://doi.org/10.1038/s41579-022-00776-z.

10. Frey, S.E., Wald, A., Edupuganti, S., Jackson, L.A., Stapleton, J.T., El Sahly, H., El-Kamary, S.S., Edwards, K., Keyserling, H., Winokur, P., et al. (2015). Comparison of lyophilized versus liquid modified vaccinia Ankara (MVA) formulations and subcutaneous versus intradermal routes of administration in healthy vaccinia-naive subjects. Vaccine *33*, 5225–5234. https://doi.org/10.1016/j.vaccine.2015.06.075.

11. Pittman, P.R., Hahn, M., Lee, H.S., Koca, C., Samy, N., Schmidt, D., Hornung, J., Weidenthaler, H., Heery, C.R., Meyer, T.P.H., et al. (2019). Phase 3 efficacy trial of modified vaccinia Ankara as a vaccine against smallpox. N. Engl. J. Med. *381*, 1897–1908. https://doi.org/10.1056/NEJMoa1817307.

12. Zhu, J., Yamane, H., and Paul, W.E. (2010). Differentiation of effector CD4 T cell populations (*). Annu. Rev. Immunol. *28*, 445–489. https://doi.org/10.1146/annurev-immunol-030409-101212.

13. Marshall, H.D., Chandele, A., Jung, Y.W., Meng, H., Poholek, A.C., Parish, I.A., Rutishauser, R., Cui, W., Kleinstein, S.H., Craft, J., and Kaech, S.M. (2011). Differential expression of Ly6C and T-bet distinguish effector and memory Th1 CD4(+) cell properties during viral infection. Immunity *35*, 633–646. https://doi.org/10.1016/j.immuni.2011.08.016.

14. Crotty, S. (2011). Follicular helper CD4 T cells (TFH). Annu. Rev. Immunol. *29*, 621–663. https://doi.org/10.1146/annurev-immunol-031210-101400.

15. Künzli, M., Schreiner, D., Pereboom, T.C., Swarnalekha, N., Litzler, L.C., Lötscher, J., Ertuna, Y.I., Roux, J., Geier, F., Jakob, R.P., et al. (2020). Long-lived T follicular helper cells retain plasticity and help sustain humoral immunity. Sci. Immunol. *5*, eaay5552. https://doi.org/10.1126/sciimmunol.aay5552.

16. Swain, S.L., McKinstry, K.K., and Strutt, T.M. (2012). Expanding roles for CD4(+) T cells in immunity to viruses. Nat. Rev. Immunol. *12*, 136–148. https://doi.org/10.1038/nri3152.

17. Maloy, K.J., Burkhart, C., Junt, T.M., Odermatt, B., Oxenius, A., Piali, L., Zinkernagel, R.M., and Hengartner, H. (2000). CD4(+) T cell subsets during

virus infection Protective capacity depends on effector cytokine secretion and on migratory capability. J. Exp. Med. *191*, 2159–2170. https://doi.org/10.1084/jem.191.12.2159.

18. Byun, M., Wang, X., Pak, M., Hansen, T.H., and Yokoyama, W.M. (2007). Cowpox virus exploits the endoplasmic reticulum retention pathway to inhibit MHC class I transport to the cell surface. Cell Host Microbe *2*, 306–315. https://doi.org/10.1016/j.chom.2007.09.002.

19. Alzhanova, D., Edwards, D.M., Hammarlund, E., Scholz, I.G., Horst, D., Wagner, M.J., Upton, C., Wiertz, E.J., Slifka, M.K., and Früh, K. (2009). Cowpox virus inhibits the transporter associated with antigen processing to evade T cell recognition. Cell Host Microbe *6*, 433–445. https://doi.org/10.1016/j.chom.2009.09.013.

20. Hammarlund, E., Dasgupta, A., Pinilla, C., Norori, P., Früh, K., and Slifka, M.K. (2008). Monkeypox virus evades antiviral CD4+ and CD8+ T cell responses by suppressing cognate T cell activation. Proc. Natl. Acad. Sci. USA *105*, 14567–14572. https://doi.org/10.1073/pnas.0800589105.

21. Gainey, M.D., Rivenbark, J.G., Cho, H., Yang, L., and Yokoyama, W.M. (2012). Viral MHC class I inhibition evades CD8+ T-cell effector responses in vivo but not CD8+ T-cell priming. Proc. Natl. Acad. Sci. USA *109*, E3260–E3267. https://doi.org/10.1073/pnas.1217111109.

22. Lauron, E.J., Yang, L., Harvey, I.B., Sojka, D.K., Williams, G.D., Paley, M.A., Bern, M.D., Park, E., Victorino, F., Boon, A.C.M., and Yokoyama, W.M. (2019). Viral MHCI inhibition evades tissue-resident memory T cell formation and responses. J. Exp. Med. *216*, 117–132. https://doi.org/10.1084/jem.20181077.

23. Simpson, C.L., Patel, D.M., and Green, K.J. (2011). Deconstructing the skin: cytoarchitectural determinants of epidermal morphogenesis. Nat. Rev. Mol. Cell Biol. *12*, 565–580. https://doi.org/10.1038/nrm3175.

24. Klicznik, M.M., Szenes-Nagy, A.B., Campbell, D.J., and Gratz, I.K. (2018). Taking the lead - how keratinocytes orchestrate skin T cell immunity. Immunol. Lett. *200*, 43–51. https://doi.org/10.1016/j.imlet.2018.06.009.

25. Kashiwagi, M., Hosoi, J., Lai, J.F., Brissette, J., Ziegler, S.F., Morgan, B.A., and Georgopoulos, K. (2017). Direct control of regulatory T cells by keratinocytes. Nat. Immunol. *18*, 334–343. https://doi.org/10.1038/ni.3661.

26. Aluwihare, P., Mu, Z., Zhao, Z., Yu, D., Weinreb, P.H., Horan, G.S., Violette, S.M., and Munger, J.S. (2009). Mice that lack activity of alphavbeta6- and alphavbeta8-integrins reproduce the abnormalities of Tgfb1- and Tgfb3-null mice. J. Cell Sci. *122*, 227–232. https://doi.org/10.1242/jcs.035246.

27. Lei, V., Petty, A.J., Atwater, A.R., Wolfe, S.A., and MacLeod, A.S. (2020). Skin viral infections: host antiviral innate immunity and viral immune evasion. Front. Immunol. *11*, 593901. https://doi.org/10.3389/fimmu.2020.593901.

28. Buller, R.M., Smith, G.L., Cremer, K., Notkins, A.L., and Moss, B. (1985). Decreased virulence of recombinant vaccinia virus expression vectors is associated with a thymidine kinase-negative phenotype. Nature *317*, 813–815. https://doi.org/10.1038/317813a0.

29. Moutaftsi, M., Bui, H.H., Peters, B., Sidney, J., Salek-Ardakani, S., Oseroff, C., Pasquetto, V., Crotty, S., Croft, M., Lefkowitz, E.J., et al. (2007). Vaccinia virus-specific CD4+ T cell responses target a set of antigens largely distinct from those targeted by CD8+ T cell responses. J. Immunol. *178*, 6814–6820. https://doi.org/10.4049/jimmunol.178.11.6814.

30. Tscharke, D.C., Karupiah, G., Zhou, J., Palmore, T., Irvine, K.R., Haeryfar, S.M.M., Williams, S., Sidney, J., Sette, A., Bennink, J.R., and Yewdell, J.W. (2005). Identification of poxvirus CD8+ T cell determinants to enable rational design and characterization of smallpox vaccines. J. Exp. Med. *201*, 95–104. https://doi.org/10.1084/jem.20041912.

31. Hobbs, S.J., Harbour, J.C., Yates, P.A., Ortiz, D., Landfear, S.M., and Nolz, J.C. (2020). Vaccinia virus vectors targeting peptides for MHC class II presentation to CD4(+) T cells. Immunohorizons *4*, 1–13. https://doi.org/10.4049/immunohorizons.1900070.

32. Nolz, J.C., and Harty, J.T. (2014). IL-15 regulates memory CD8+ T cell O-glycan synthesis and affects trafficking. J. Clin. Invest. *124*, 1013–1026. https://doi.org/10.1172/JCI72039.

33. Hobbs, S.J., and Nolz, J.C. (2017). Regulation of T Cell trafficking by enzymatic synthesis of O-glycans. Front. Immunol. *8*, 600. https://doi.org/10.3389/fimmu.2017.00600.

34. Priatel, J.J., Chui, D., Hiraoka, N., Simmons, C.J., Richardson, K.B., Page, D.M., Fukuda, M., Varki, N.M., and Marth, J.D. (2000). The ST3Gal-I sialyltransferase controls CD8+ T lymphocyte homeostasis by modulating O-glycan biosynthesis. Immunity *12*, 273–283.

35. Carlow, D.A., Gossens, K., Naus, S., Veerman, K.M., Seo, W., and Ziltener, H.J. (2009). PSGL-1 function in immunity and steady state homeostasis. Immunol. Rev. *230*, 75–96. https://doi.org/10.1111/j.1600-065X.2009.00797.x.

36. Hickman, H.D., Reynoso, G.V., Ngudiankama, B.F., Rubin, E.J., Magadán, J.G., Cush, S.S., Gibbs, J., Molon, B., Bronte, V., Bennink, J.R., and Yewdell, J.W. (2013). Anatomically restricted synergistic antiviral activities of innate and adaptive immune cells in the skin. Cell Host Microbe *13*, 155–168. https://doi.org/10.1016/j.chom.2013.01.004.

37. Nagao, K., Kobayashi, T., Moro, K., Ohyama, M., Adachi, T., Kitashima, D.Y., Ueha, S., Horiuchi, K., Tanizaki, H., Kabashima, K., et al. (2012). Stress-induced production of chemokines by hair follicles regulates the trafficking of dendritic cells in skin. Nat. Immunol. *13*, 744–752. https://doi.org/10.1038/ni.2353.

38. Khan, T.N., Mooster, J.L., Kilgore, A.M., Osborn, J.F., and Nolz, J.C. (2016). Local antigen in nonlymphoid tissue promotes resident memory CD8+ T cell formation during viral infection. J. Exp. Med. *213*, 951–966. https://doi.org/10.1084/jem.20151855.

39. Schoggins, J.W. (2019). Interferon-stimulated genes: what do they all do? Annu. Rev. Virol. *6*, 567–584. https://doi.org/10.1146/annurev-virology-092818-015756.

40. Tubo, N.J., and Jenkins, M.K. (2014). CD4+ T Cells: guardians of the phagosome. Clin. Microbiol. Rev. *27*, 200–213. https://doi.org/10.1128/CMR.00097-13.

41. Knudson, C.J., Férez, M., Alves-Peixoto, P., Erkes, D.A., Melo-Silva, C.R., Tang, L., Snyder, C.M., and Sigal, L.J. (2021). Mechanisms of antiviral cytotoxic CD4 T cell differentiation. J. Virol. *95*, e0056621. https://doi.org/10.1128/JVI.00566-21.

42. Krueger, P.D., Goldberg, M.F., Hong, S.W., Osum, K.C., Langlois, R.A., Kotov, D.I., Dileepan, T., and Jenkins, M.K. (2021). Two sequential activation modules control the differentiation of protective T helper-1 (Th1) cells. Immunity *54*, 687–701.e4. https://doi.org/10.1016/j.immuni.2021.03.006.

43. Penaloza-MacMaster, P., Barber, D.L., Wherry, E.J., Provine, N.M., Teigler, J.E., Parenteau, L., Blackmore, S., Borducchi, E.N., Larocca, R.A., Yates, K.B., et al. (2015). Vaccine-elicited CD4 T cells induce immunopathology after chronic LCMV infection. Science *347*, 278–282. https://doi.org/10.1126/science.aaa2148.

44. Knudson, C.J., Hartwig, S.M., Meyerholz, D.K., and Varga, S.M. (2015). RSV vaccine-enhanced disease is orchestrated by the combined actions of distinct CD4 T cell subsets. PLoS Pathog. *11*, e1004757. https://doi.org/10.1371/journal.ppat.1004757.

45. Teo, T.H., Lum, F.M., Claser, C., Lulla, V., Lulla, A., Merits, A., Rénia, L., and Ng, L.F.P. (2013). A pathogenic role for CD4+ T cells during Chikungunya virus infection in mice. J. Immunol. *190*, 259–269. https://doi.org/10.4049/jimmunol.1202177.

46. Stohlman, S.A., Hinton, D.R., Parra, B., Atkinson, R., and Bergmann, C.C. (2008). CD4 T cells contribute to virus control and pathology following central nervous system infection with neurotropic mouse hepatitis virus. J. Virol. *82*, 2130–2139. https://doi.org/10.1128/JVI.01762-07.

47. Anghelina, D., Pewe, L., and Perlman, S. (2006). Pathogenic role for virus-specific CD4 T cells in mice with coronavirus-induced acute encephalitis. Am. J. Pathol. *169*, 209–222. https://doi.org/10.2353/ajpath.2006.051308.

48. Brown, D.M., Dilzer, A.M., Meents, D.L., and Swain, S.L. (2006). CD4 T cell-mediated protection from lethal influenza: perforin and antibody-mediated mechanisms give a one-two punch. J. Immunol. *177*, 2888–2898. https://doi.org/10.4049/jimmunol.177.5.2888.

49. Strutt, T.M., McKinstry, K.K., Dibble, J.P., Winchell, C., Kuang, Y., Curtis, J.D., Huston, G., Dutton, R.W., and Swain, S.L. (2010). Memory CD4+ T cells induce innate responses independently of pathogen. Nat. Med. *16*, 558–564. https://doi.org/10.1038/nm.2142.

50. Chapman, T.J., Lambert, K., and Topham, D.J. (2011). Rapid reactivation of extralymphoid CD4 T cells during secondary infection. PLoS One *6*, e20493. https://doi.org/10.1371/journal.pone.0020493.

51. Son, Y.M., Cheon, I.S., Wu, Y., Li, C., Wang, Z., Gao, X., Chen, Y., Takahashi, Y., Fu, Y.X., Dent, A.L., et al. (2021). Tissue-resident CD4(+) T helper cells assist the development of protective respiratory B and CD8(+) T cell memory responses. Sci. Immunol. *6*, eabb6852. https://doi.org/10.1126/sciimmunol.abb6852.

52. Swarnalekha, N., Schreiner, D., Litzler, L.C., Iftikhar, S., Kirchmeier, D., Künzli, M., Son, Y.M., Sun, J., Moreira, E.A., and King, C.G. (2021). T resident helper cells promote humoral responses in the lung. Sci. Immunol. *6*, eabb6808. https://doi.org/10.1126/sciimmunol.abb6808.

53. Osborn, J.F., Hobbs, S.J., Mooster, J.L., Khan, T.N., Kilgore, A.M., Harbour, J.C., and Nolz, J.C. (2019). Central memory CD8+ T cells become CD69+ tissue-residents during viral skin infection independent of CD62L-mediated lymph node surveillance. PLoS Pathog. *15*, e1007633. https://doi.org/10.1371/journal.ppat.1007633.

54. Osborn, J.F., Mooster, J.L., Hobbs, S.J., Munks, M.W., Barry, C., Harty, J.T., Hill, A.B., and Nolz, J.C. (2017). Enzymatic synthesis of core 2 O-glycans governs the tissue-trafficking potential of memory CD8(+) T cells. Sci. Immunol. *2*, eaan6049. https://doi.org/10.1126/sciimmunol.aan6049.

55. Underhill, G.H., Zisoulis, D.G., Kolli, K.P., Ellies, L.G., Marth, J.D., and Kansas, G.S. (2005). A crucial role for T-bet in selectin ligand expression in T helper 1 (Th1) cells. Blood *106*, 3867–3873. https://doi.org/10.1182/blood-2005-03-0984.

56. Tamoutounour, S., Han, S.J., Deckers, J., Constantinides, M.G., Hurabielle, C., Harrison, O.J., Bouladoux, N., Linehan, J.L., Link, V.M., Vujkovic-Cvijin, I., et al. (2019). Keratinocyte-intrinsic MHCII expression controls microbiota-induced Th1 cell responses. Proc. Natl. Acad. Sci. USA *116*, 23643–23652. https://doi.org/10.1073/pnas.1912432116.

57. Carr, M.M., McVittie, E., Guy, K., Gawkrodger, D.J., and Hunter, J.A. (1986). MHC class II antigen expression in normal human epidermis. Immunology *59*, 223–227.

58. Norbury, C.C., Malide, D., Gibbs, J.S., Bennink, J.R., and Yewdell, J.W. (2002). Visualizing priming of virus-specific CD8+ T cells by infected dendritic cells in vivo. Nat. Immunol. *3*, 265–271. https://doi.org/10.1038/ni762.

59. Baldridge, M.T., Lee, S., Brown, J.J., McAllister, N., Urbanek, K., Dermody, T.S., Nice, T.J., and Virgin, H.W. (2017). Expression of Ifnlr1 on intestinal epithelial cells is critical to the antiviral effects of interferon lambda against norovirus and reovirus. J. Virol. *91*, e02079-16. https://doi.org/10.1128/JVI.02079-16.

60. Yang, J., Hirata, T., Croce, K., Merrill-Skoloff, G., Tchernychev, B., Williams, E., Flaumenhaft, R., Furie, B.C., and Furie, B. (1999). Targeted gene disruption demonstrates that P-selectin glycoprotein ligand 1 (PSGL-1) is required for P-selectin-mediated but not E-selectin-mediated neutrophil rolling and migration. J. Exp. Med. *190*, 1769–1782. https://doi.org/10.1084/jem.190.12.1769.

61. Reinhardt, R.L., Liang, H.E., and Locksley, R.M. (2009). Cytokine-secreting follicular T cells shape the antibody repertoire. Nat. Immunol. *10*, 385–393. https://doi.org/10.1038/ni.1715.

62. Lee, S.H., Carrero, J.A., Uppaluri, R., White, J.M., Archambault, J.M., Lai, K.S., Chan, S.R., Sheehan, K.C.F., Unanue, E.R., and Schreiber, R.D. (2013). Identifying the initiating events of anti-Listeria responses using mice with conditional loss of IFN-gamma receptor subunit 1 (IFNGR1). J. Immunol. *191*, 4223–4234. https://doi.org/10.4049/jimmunol.1300910.

63. Hashimoto, K., Joshi, S.K., and Koni, P.A. (2002). A conditional null allele of the major histocompatibility IA-beta chain gene. Genesis *32*, 152–153. https://doi.org/10.1002/gene.10056.

64. Van Keymeulen, A., Rocha, A.S., Ousset, M., Beck, B., Bouvencourt, G., Rock, J., Sharma, N., Dekoninck, S., and Blanpain, C. (2011). Distinct stem cells contribute to mammary gland development and maintenance. Nature *479*, 189–193. https://doi.org/10.1038/nature10573.

65. Oxenius, A., Bachmann, M.F., Zinkernagel, R.M., and Hengartner, H. (1998). Virus-specific MHC-class II-restricted TCR-transgenic mice: effects on humoral and cellular immune responses after viral infection. Eur. J. Immunol. *28*, 390–400.

66. Durbin, J.E., Hackenmiller, R., Simon, M.C., and Levy, D.E. (1996). Targeted disruption of the mouse Stat1 gene results in compromised innate immunity to viral disease. Cell *84*, 443–450. https://doi.org/10.1016/s0092-8674(00)81289-1.

67. Müller, U., Steinhoff, U., Reis, L.F., Hemmi, S., Pavlovic, J., Zinkernagel, R.M., and Aguet, M. (1994). Functional role of type I and type II interferons in antiviral defense. Science *264*, 1918–1921. https://doi.org/10.1126/science.8009221.

68. Dobin, A., Davis, C.A., Schlesinger, F., Drenkow, J., Zaleski, C., Jha, S., Batut, P., Chaisson, M., and Gingeras, T.R. (2013). STAR: ultrafast universal RNA-seq aligner. Bioinformatics *29*, 15–21. https://doi.org/10.1093/bioinformatics/bts635.

69. Love, M.I., Huber, W., and Anders, S. (2014). Moderated estimation of fold change and dispersion for RNA-seq data with DESeq2. Genome Biol. *15*, 550. https://doi.org/10.1186/s13059-014-0550-8.

70. Young, M.D., Wakefield, M.J., Smyth, G.K., and Oshlack, A. (2010). Gene ontology analysis for RNA-seq: accounting for selection bias. Genome Biol. *11*, R14. https://doi.org/10.1186/gb-2010-11-2-r14.

71. Afgan, E., Baker, D., Batut, B., van den Beek, M., Bouvier, D., Cech, M., Chilton, J., Clements, D., Coraor, N., Grüning, B.A., et al. (2018). The Galaxy platform for accessible, reproducible and collaborative biomedical analyses: 2018 update. Nucleic Acids Res. *46*, W537–W544. https://doi.org/10.1093/nar/gky379.

72. Subramanian, A., Tamayo, P., Mootha, V.K., Mukherjee, S., Ebert, B.L., Gillette, M.A., Paulovich, A., Pomeroy, S.L., Golub, T.R., Lander, E.S., and Mesirov, J.P. (2005). Gene set enrichment analysis: a knowledge-based approach for interpreting genome-wide expression profiles. Proc. Natl. Acad. Sci. USA *102*, 15545–15550. https://doi.org/10.1073/pnas.0506580102.

73. Liberzon, A., Birger, C., Thorvaldsdóttir, H., Ghandi, M., Mesirov, J.P., and Tamayo, P. (2015). The Molecular Signatures Database (MSigDB) hallmark gene set collection. Cell Syst. *1*, 417–425. https://doi.org/10.1016/j.cels.2015.12.004.

STAR★METHODS

KEY RESOURCES TABLE

REAGENT or RESOURCE	SOURCE	IDENTIFIER
Antibodies		
IgG from rat serum	Sigma-Aldrich	#I4131
InVivoMAb anti-mouse CD4 (clone GK1.5)	Bio X Cell	Cat#BE0003
InVivoMAb anti-mouse CD8α (clone 2.43)	Bio X Cell	Cat#BE0061
InVivoMAb anti-mouse IFNγ (clone XMG1.2)	Bio X Cell	Cat#BE0055
Rat anti-mouse P-selectin blocking antibody (clone RB40)	Purified from hybridoma in house	N/A
Rat anti-mouse E-selectin blocking antibody (clone 9A9)	Purified from hybridoma in house	N/A
PE anti-mouse CD197 (CCR7) Antibody (clone 4B12)	BioLegend	Cat#120106; RRID: AB_389358
Biotin anti-mouse CD119 (IFNγR α-Chain) Antibody (clone 2E2)	BioLegend	Cat#112804; RRID: AB_2123475
PE anti-mouse CD122 Antibody (clone 5H4)	BioLegend	Cat#105906; RRID: AB_2125736
InVivoMAb anti-mouse CD16/CD32 (clone 2.4G2)	Bio X Cell	Cat#BE0307; RRID: AB_2736987
FITC anti-mouse CD34 (clone RAM34)	Invitrogen/eBioscience	Cat#11-0341-82; RRID: AB_465021
APC anti-mouse CD4 Antibody (clone RM4-5)	BioLegend	Cat#100516; RRID: AB_312719
FITC anti-mouse CD43 Activation-Associated Glycoform Antibody (clone 1B11)	BioLegend	Cat#121206; RRID: AB_493386
Pacific Blue anti-mouse/human CD44 Antibody (clone 1M7)	BioLegend	Cat#103020; RRID: AB_493683
PE/Cyanine7 anti-mouse CD45.2 Antibody (clone 104)	BioLegend	Cat#109830; RRID: AB_1186098
APC anti-mouse CD8α Antibody (clone 53–6.7)	BioLegend	Cat#100712; RRID: AB_312751
PE Goat anti-Human IgG Fc (polyclonal)	Invitrogen/eBioscience	Cat#12-4998-82; RRID: AB_465926
APC anti-mouse IFNγ Antibody (clone XMG1.2)	BioLegend	Cat#505810; RRID: AB_315404
PE anti-mouse I-A^b Antibody (clone AF6-120.1)	BioLegend	Cat#116408; RRID: AB_313727
PE anti-mouse I-A/I-E Antibody (clone M5/114.15.2)	BioLegend	Cat#107608; RRID: AB_313323
Pacific Blue anti-mouse Ly6C Antibody (clone HK1.4)	BioLegend	Cat#128014; RRID: AB_1732079
PE MHC Class I (H-2Kd/H-2Dd) Monoclonal Antibody (clone 34-1-2S)	Invitrogen	Cat#12-5998-82; RRID: AB_466122
PE Rat anti-mouse CD162 (PSGL-1) (clone 2PH1)	BD Biosciences	Cat#555306; RRID: AB_395719
PE Rat IgG2a, k Isotype Ctrl Antibody (clone RTK2758)	BioLegend	Cat#400508; RRID: AB_326530
APC anti-mouse Ly-6A/E (Sca-1) Antibody (clone E13–161.7)	BioLegend	Cat#122512; RRID: AB_756197
Brilliant Violet 711 anti-rat CD90/mouse CD90.1 (Thy-1.1) Antibody (clone OX-7)	BioLegend	Cat#202539; RRID: AB_2562645
FITC anti-mouse TNFα Antibody (clone MP6-XT22)	BioLegend	Cat#506304; RRID: AB_315425
Bacterial and virus strains		
Lymphocytic choriomeningitis virus (LCMV) Armstrong	N/A	N/A
Vaccinia Virus (VacV) Western Reserve	BEI Resources	NR-55
Modified Vaccinia virus Ankara (MVA)	BEI Resources	NR-1
Cowpox Virus (CPXV) Brighton Red Strain	Klaus Früh	N/A
CPXVΔ203 Brighton Red Strain	Klaus Früh (originally from Wayne Yokoyama)	Byun et al.[18]

(Continued on next page)

Continued

REAGENT or RESOURCE	SOURCE	IDENTIFIER
VacV (*tk*- expressing β-Galactosidase)	Ann Hill	N/A
VacV-NP-S-eGFP	Jon Yewdell and Jack Bennick	Norbury et al.[58]
VacV-li-GP$_{61-80}$ (VacV-GP61)	Generated in the Nolz Laboratory	Hobbs et al.[31]
Chemicals, peptides, and recombinant proteins		
Tamoxifen Supplemented Diet (TAM Diet (500, 2016)) -Irradiated	Envigo	TD.130857
SeaPlaque Agarose	Lonza	Cat#50100
2x Modified Eagle Medium	Gibco	Cat#11935046
Neutral Red dye	Sigma-Aldrich	CAS#553-24-2
HBSS Modified	Gibco	Cat#SH3003103
Collagenase II	Gibco	Cat#17101015
DNase-I	Sigma-Aldrich	CAS#9003-98-9
Percoll	Cytiva	Cat#17089101
Dispase II	Sigma-Aldrich	CAS#42613-33-2
Trypsin-EDTA (0.25%)	Gibco	Cat#25200056
I-A^b-GP$_{61-80}$	NIH Tetramer Core Facility	IEDB ID: 175783 Uniprot ID: P09991
I-A^b-CLIP$_{87-101}$	NIH Tetramer Core Facility	IEDB ID: 119507 Uniprot ID: P04233
Recombinant Mouse P-Selectin/CD62P Fc Chimera Protein, CF	R & D Systems	Cat#737-PS-050
Recombinant Mouse E-Selectin/CD62E Fc Chimera Protein, CF	R & D Systems	Cat#575-ES-100
eBioscience Streptavidin PE Conjugate	Invitrogen/eBioscience	Cat#12-4317-87
Ghost Dye Red 780 Viability Dye	Tonbo biosciences	Cat#13-0865-T100
Peanut Agglutinin (PNA) Fluorescein	Vector Laboratories Inc.	Cat#FL-1071
Cytofix/Cytoperm buffer	BD Biosciences	Cat#554722
Vitalyse 10X lysing buffer	CytoMedical Design Group, LLC	WBL0100
Brefeldin A	BioLegend	Cat#420601
Perm/Wash buffer I	BD Biosciences	Cat#557885
Power SYBR green PCR Master Mix	Applied Biosystems	Cat#4368577
SuperScript First-Strand Synthesis System	Invitrogen	Cat#18091050
Peptide: GP$_{33-41}$: KAVYNFATC	Bio-synthesis, Inc.	14770–01
Peptide: GP$_{61-80}$: GLKGPDIYKGVYQFKSVEFD	Bio-synthesis, Inc.	14258–01
Peptide I1L$_{7-21}$: QLVFNSISARALKAY	Bio-synthesis, Inc.	Custom Order
Peptide L4R$_{173-187}$: ISKYAGINILNVYSP	Bio-synthesis, Inc.	Custom Order
Peptide H3L$_{269-283}$: PGVMYTFTTPLISFF	Bio-synthesis, Inc.	Custom Order
Experimental models: Cell lines		
BSC-40	ATCC	CRL-2761
Experimental models: Organisms/strains		
Mouse: C57BL/6N	Charles River/National Cancer Institute	Strain Code: 027
Mouse: C57Bl/6J	The Jackson Laboratory	Strain#:000664
Mouse: *Selplg*$^{-/-}$	The Jackson Laboratory	Strain #:004201
Mouse: interferon-gamma reporter with endogenous polyA transcript (GREAT; IFNg-YFP)	The Jackson Laboratory	Strain #:017581
Mouse: *Ifngr1*^{f}	The Jackson Laboratory	Strain #:025394
Mouse: *H2-Ab1*-flox	The Jackson Laboratory	Strain #:013181
Mouse: K5-CreER^{T2}	The Jackson Laboratory	Strain #:029155
Mouse: K14-Cre	The Jackson Laboratory	Strain #:018964

(Continued on next page)

Continued

REAGENT or RESOURCE	SOURCE	IDENTIFIER
Mouse: SMARTA TCR-transgenic (TCR-tg)	The Jackson Laboratory	Strain #:030450
Mouse: *Stat1*$^{-/-}$	The Jackson Laboratory	Strain #:012606
Mouse: *Ifnlr1*$^{-/-}$	Tim Nice	Baldridge et al.[59]
Mouse: *Ifnar1*$^{-/-}$	Tim Nice	MMRRC Strain #032045-JAX
Oligonucleotides		
See Table S1 for qPCR primers used	This Paper	N/A
Deposited data		
RNA sequencing data	This paper	GEO: GSE227917
Software and algorithms		
FlowJo Software (versions 10.5.3, 10.7.2, or 9.9.6)	BD Biosciences	https://www.flowjo.com/solutions/flowjo
Prism Software (GraphPad Software)	GraphPad	https://www.graphpad.com/features
Galaxy		https://usegalaxy.org/
Other		
25M Pocket Thickness Gauge Measure	Ames	Series 25

RESOURCE AVAILABILITY

Lead contact

Further information and requests for resources and reagents should be directed to and will be fulfilled by the lead contact, Jeffrey Nolz (nolz@ohsu.edu).

Materials availability

This study did not generate new unique reagents.

Data and code availability

- RNA-seq data generated in this study have been deposited in the Gene Expression Omnibus, accession number GSE227917.
- This paper does not report original code.
- Any additional information required to reanalyze the data reported in this paper is available from the lead contact upon request.

EXPERIMENTAL MODEL AND SUBJECT DETAILS

Mice

All mice in this study were housed and bred under specific pathogen-free conditions at Oregon Health & Science University. C57BL/6N and C57BL/6J mice (6–8 weeks of age) were purchased from Charles River/National Cancer Institute and The Jackson Laboratory, respectively. *Selplg*$^{-/-}$,[60] interferon-gamma reporter with endogenous polyA transcript (GREAT; IFNγ-YFP),[61] *Ifngr1*^{f},[62] *H2-Ab1*-flox,[63] K5-CreER^{T2},[64] and K14-Cre mice were purchased from The Jackson Laboratory. SMARTA TCR-transgenic (TCR-tg) mice have been described previously and maintained by sibling x sibling mating.[65] SMARTA TCR-tg IFNγ-YFP mice were generated by mating homozygous GREAT mice to SMARTA mice to generate SMARTA-TCR-tg mice expressing one copy of the IFNγ-YFP reporter. *Stat1*$^{-/-}$ mice have been previously described.[66] *Ifnlr1*$^{-/-}$[59] and *Ifnar1*$^{-/-}$[67] double knockout mice were bred to *Ifnlr1*$^{-/+}$/ *Ifnar1*$^{-/+}$ double heterozygous mice to generate littermate offspring. *H2-Ab1*$^{fl/fl}$ K5-CreER^{T2} (+/−) mice were provided *ad libitum* a tamoxifen supplemented diet (Envigo) for 7 days. Littermate controls (both males and females) were used for all experiments. For T cell transfers, SMARTA TCR-tg T cells (~250,000) from the spleen were injected intravenously in 200 μL of PBS. For depletion of CD4^{+} T cells and CD8^{+} T cells from the circulation, mice were given 250 μg of control rat IgG (Sigma), anti-CD4 antibody (clone GK1.5, Bio X Cell), or anti-CD8α antibody (clone 2.43, Bio X Cell) 1–3 times in 200 μL of PBS by i.p. injection. For neutralization of cytokines, mice were treated with 200 μg of control rat IgG (Sigma) or anti-IFNγ antibody (clone XMG1.2, Bio X Cell) on days 0, 2, 4, and 6 post-infection. For P and E-selectin blocking experiments, 250 μg of anti-P-selectin (clone RB40) and/or anti-E-selectin (clone 9A9) antibodies were delivered i.p. in PBS on days −1, 1 and 2 post-VacV infection. Tissue inflammation of the ear skin (swelling) was measured using a dial micrometer (Ames).

All animal experiments were approved by the OHSU Institutional Animal Care and Use Committee and Institutional Biosafety Committee.

Viruses and infections

Lymphocytic choriomeningitis virus (LCMV)-Armstrong (2×10^5 PFU) in 200 μL of PBS was delivered by i.p. injection. VacV-WR and MVA were obtained from BEI Resources. CPXV and Δ203CPXV were the Brighton Red strain and have been previously described.[18] VacV (*tk*-expressing β-Galactosidase), VacV-NP-S-eGFP, and VacV expressing the GP_{61-80} peptide from LCMV conjugated to CD74 to allow for MHC-II presentation (VacV-Ii-GP61) have been described previously.[31,58] VacV and CPXV skin infections were performed by pipetting 10 μL of PBS containing virus (5×10^5 PFU - 5×10^7 PFU for VacV and 1×10^6 PFU for CPXV) onto the ventral ear skin and poking the skin 25–35 times with a 16.5-gauge needle. MVA (1×10^7 PFU) was delivered subcutaneously in 50 μL of media.

Quantification of VacV or CPXV from infected ear skin was performed using standard plaque assays on BSC-40 cells. Briefly, infected ears were removed and homogenized in 1 mL of RPMI supplemented with 1% FBS. Skin homogenates were then subjected to three rounds of freeze-thaw before 10-fold serial dilutions were aliquoted onto BSC-40 cells in a 12-well plate, incubated at 37C for 2–3 h, and then covered with 1% Seakem agarose in Modified Eagle Medium (Gibco). Plaques were visualized 2–3 days later following overnight incubation with Neutral Red dye.

METHOD DETAILS

Leukocyte isolation from skin

Ears from infected mice were removed and the dorsal and ventral sides of the ear pinna were separated and incubated for 1–1.5 h at 37C with 1 mL HBSS (Gibco) containing $CaCl_2$ and $MgCl_2$ supplemented with 125 U/mL collagenase (Invitrogen) and 60 U/mL DNase-I (Sigma-Aldrich). Single cell suspensions were then generated by forcing the tissue through a wire mesh screen and a 70 μM-pore size filter. Leukocytes were then purified from whole tissue suspensions by re-suspending the cells in 10 mL of 35% Percoll in HBSS in 50 mL conical tubes followed by centrifugation (500 x g) for 10 min at room temp.

Isolation of epidermis for analysis of keratinocytes

Ears from mice were removed and dorsal/ventral sides of the ear pinna were separated and incubated at 37C in 2.5 mg/mL of Dispase II (Sigma-Aldrich) in PBS with Ca^{2+} and $Mg2^+$ (Gibco) for 90 min. The epidermis was then peeled away from the dermis using forceps and both the ventral and dorsal epidermis were placed in 0.25% trypsin (Gibco) for 1 h at 37C. The epidermis was then made into a single cell suspension by gently forcing the tissue through metal mesh screens and a 70 μM-pore size filter. After staining, cells were filtered a second time through a 35 μm nylon filter (Falcon) before flow cytometer analysis.

Flow cytometry and cell sorting

$I-A^b-GP_{61-80}$ and $CLIP_{87-101}$ were acquired from the NIH Tetramer Core Facility. Tetramer and CCR7 staining were performed for 45 min at 37C in FACS buffer (PBS/1% FBS/0.02% sodium azide). Staining for other surface antigens was performed in FACS buffer, 4C for 15–20 min. Cells were then washed with FACS buffer and fixed with Cytofix/Cytoperm buffer (BD Biosciences) for 10 min at 4C then washed two additional times with FACS buffer prior to analysis. To quantify P- and E-selectin binding, recombinant E-selectin (5 μg/mL) and P-selectin (1 μg/mL) human IgG Fc chimeric proteins (R & D Systems) were incubated with cells for 45 min in 1% FBS/DPBS containing Ca^{2+} and Mg^{2+} (Gibco) at room temperature. All subsequent staining steps were performed with 1% FBS/DPBS containing Ca^{2+} and Mg^{2+} at 4C and binding of selectins was detected using anti-human IgG-Fc PE (eBioscience). Data were acquired on an LSRII Flow Cytometer (BD Biosciences) or BD Symphony in the Oregon Health & Science University Flow Cytometry Core Facility. Flow cytometry data were analyzed with FlowJo Software (BD Biosciences) Versions 10.5.3, 10.7.2, or 9.9.6. To identify and sort keratinocytes, single cell suspensions were generated as described in *Epidermal Isolation for Analysis of Keratinocytes* and stained with Sca-1-APC, Viability Dye-Ghost Red 780, CD45.2-Pac Blue, and MHC-II-PE and sorted using a BD Influx Cell Sorter in the OHSU Flow Cytometry Core Facility.

Ex vivo peptide stimulation and intracellular stain

Single cell suspensions from spleens or lymph nodes were made by gently forcing the tissues through mesh metal screens. Red blood cells were lysed with 1x Vitalyse buffer (CytoMedical Design Group, LLC). Splenocytes were stimulated for 5 h with 1 μM of peptide (Bio-synthesis) in the presence of Brefeldin A (BioLegend) in RPMI 1640 medium (Gibco) containing 10% FBS at 37C. The CytoFix/CytoPerm kit (BD Biosciences) was used for intracellular cytokine stain following the manufacturer's protocol. Antibodies against surface antigens were stained for 15 min in 4C in FACS buffer, washed with FACS buffer and then permeabilized with 100 μL of Cytofix/Cytoperm for 10 min at 4C. After washing with Perm/Wash, antibodies against cytokines were incubated in Perm/Wash buffer for 20 min at 4C. Cells were then washed two times with Perm/Wash buffer and resuspended in FACS buffer for FACS analysis.

Antibodies and staining reagents

The following antibodies and staining reagents were used in this study: CD4 (RM4-5; BioLegend), CD8α (53–6.7; BioLegend), Thy1.1 (OX-7; BioLegend), CD44 (1M7; BioLegend), CD122 (5H4; BioLegend), PNA (FL-1071; Vector Laboratories Inc.), PSGL-1 (2PH1; BD Biosciences), CCR7 (4B12; BioLegend), CD43 Activation-Associated Glycoform (1B11; BioLegend), CD16/32 (2.4G2; Bio X Cell), Ly6C (HK1.4; BioLegend), Sca-1 (E13–161.7; BioLegend), CD34 (MED14.7; BioLegend), $I-A^b$ (AF6-120.1; BioLegend), MHC Class

I (34-1-25; Invitrogen), I-A/I-E (M5/114.15.2; BioLegend), CD119 (IFNγR α chain) (2E2; BioLegend), Goat anti-Human IgG Fc (Polyclonal; Invitrogen/eBioscience), eBioscience Streptavidin (Invitrogen), Rat IgG2a, κ Isotype Ctrl (RTK2758; BioLegend), Ghost Red 780 Viability Dye (Tonbo biosciences), CD45.2 (104; BioLegend), IFNγ (XMG1.2; BioLegend) and TNFα (MP6-XT22; BioLegend).

RNA sequencing and analysis

Whole ear skin was homogenized in 1 mL of Trizol and RNA was extracted according to the manufacturers protocol. RNA was further purified using the RNeasy Mini Kit (Qiagen). RNA integrity was determined by running samples on the Bioanalyzer (Agilent). Libraries were prepared using the TruSeq Stranded mRNA kit (Illumina). Briefly, RNA was converted to cDNA using random hexamers. Synthesis of the second strand was done with the addition of dUTP, which enforced the stranded orientation of the libraries by blocking amplification off the second strand during the first round of PCR. Amplified libraries were profiled on the 4200 TapeStation (Agilent). Libraries were quantified for sequencing using an NGS Library Quantification Kit (Roche/Kapa Biosystems) on a StepOnePlus Real-Time PCR Workstation (Thermo/ABI). Sequencing was done on a NovaSeq 6000 (Illumina). Fastq files were generated from base-call files using bcl2fastq (Illumina). The aligned read counts of gene expressions were quantified by STAR and differentially expressed genes were identified by DESeq2.[68,69] Principal component analysis was performed in DESeq2 using the normalized counts. Heat maps were generated by creating Z score values from normalized counts, where $z_{i,j} = (x_{i,j} - x_{imean})/s_i$. Only significantly differentially expressed genes (adjusted $p < 0.05$) with an overall fold change in gene expression of >2 were included and hierarchical clustering using Euclidean distance, complete linkage, and clustering of rows and columns was performed using the Morpheus webtool (Broad Institute, https://software.broadinstitute.org/morpheus). The volcano plot was generated in Prism. Gene ontology analysis was done using the GoSeq function in Galaxy using a 'gene lengths' file and a 'differentially expressed genes' file with a Boolean label of adjusted p values <0.05, labeled 'true' if the p value was <0.05 or 'false' if the p value was >0.05.[70,71] We acknowledge our use of the gene set enrichment analysis, GSEA software, and Molecular Signature Database (MSigDB).[72,73] The number of permutations were 1000 for each gene set database.

Quantitative PCR

RNA from whole ear skin was isolated as described in *RNA Sequencing and analysis* or from sorted keratinocytes as described in *Flow Cytometry and Cell Sorting*. cDNA was synthesized using the SuperScript First-Strand Synthesis System (Thermo Fisher Scientific) according to manufacturer's instructions. qPCR reactions were performed using Power SYBR green PCR Master Mix (ThermoFisher) and analyzed on a Step One Plus Real-Time PCR system (Applied Biosystems). Changes in gene expression were quantified using the $\Delta\Delta$Ct method, using expression of TATA binding protein (TBP) for normalization. In some cases, standard deviations and means were calculated using all $\Delta\Delta$Ct for a given gene to generate z-scores.

QUANTIFICATION AND STATISTICAL ANALYSIS

Statistical analyses

Data are shown as mean ± SD and/or as individual biological replicates in all graphs. Statistical analyses were performed with Prism software (GraphPad Software) using either the paired or unpaired Student's t test or ANOVA with Tukey's post-test for significance.